

# Worldwide Distribution of Geomagnetic Tides

S. R. C. Malin

*Phil. Trans. R. Soc. Lond. A* 1973 **274**, 551-594

doi: 10.1098/rsta.1973.0076

## Email alerting service

Receive free email alerts when new articles cite this article - sign up in the box at the top right-hand corner of the article or click [here](#)

To subscribe to *Phil. Trans. R. Soc. Lond. A* go to: <http://rsta.royalsocietypublishing.org/subscriptions>

## WORLDWIDE DISTRIBUTION OF GEOMAGNETIC TIDES

BY S. R. C. MALIN

*Geomagnetism Unit, Institute of Geological Sciences, Herstmonceux Castle, Hailsham, Sussex**(Communicated by W. Bullerwell, F.R.S. – Received 2 November 1972)*

## CONTENTS

	PAGE
1. INTRODUCTION	552
2. DATA AND ANALYSIS	554
2.1. Preliminary considerations	554
2.2. The data	554
2.3. Editing	555
2.4. Method of analysis	555
2.5. The analysis	557
3. DETERMINATION AND REMOVAL OF THE OCEAN DYNAMO EFFECT	561
3.1. The method	561
3.2. Application to worldwide observatories	564
4. WORLDWIDE REPRESENTATION OF THE IONOSPHERIC PART OF $L$	566
4.1. Choice of method	566
4.2. Development	570
4.3. The spherical harmonic analysis	572
4.4. Comparison with previous analyses	576
4.4.1. Methods and data	576
4.4.2. Results	578
5. THE ASSOCIATED CURRENT FUNCTIONS	580
5.1. Method	580
5.2. Results	580
5.3. Comparison with earlier current functions	581
APPENDIX A. SPHERICAL HARMONIC ANALYSIS OF THE SOLAR DAILY GEOMAGNETIC VARIATIONS	585
APPENDIX B. SPHERICAL HARMONIC ANALYSIS OF THE LUNAR SEMIDIURNAL TIDE IN THE ATMOSPHERIC PRESSURE	589
REFERENCES	593

Geomagnetic lunar-daily variations result from the Moon's tidal action on the ionosphere and oceans. They provide information that bears on the general large-scale dynamics of the atmosphere, and can also add to our understanding of ionospheric processes. For these reasons the variations, though small, are worth determining from geomagnetic data.

The data for this study are hourly mean values of the geomagnetic elements from 100 observatories for the interval 1957.5 to 1960.0. These are analysed by the Chapman–Miller method to obtain parameters of the principal lunar harmonics.

For each observatory, the contribution of the sea tidal dynamo to these parameters is empirically determined; this contribution has been ignored in previous worldwide studies, but is shown here to be an appreciable proportion of the total lunar effect, and worthy of study in its own right. After removal of the ocean dynamo effect, the remaining geomagnetic lunar daily variation, ascribed to the ionospheric dynamo and its associated induced currents, is represented by a series of spherical harmonic coefficients, and separated into parts of internal and external origin. (In this context, the relative merits of spherical harmonic analysis and the Price–Wilkins method of analysis are discussed.) Internal and external current systems associated with the ionospheric dynamo effect are deduced.

Similar analyses, for the solar daily geomagnetic variation and for the lunar semidiurnal tide in the atmospheric pressure, are appended.

## 1. INTRODUCTION

Just as tides are raised in the ocean by the gravitational influence of the Moon, so similar tides are raised in the atmosphere. The lunar daily atmospheric tide is dwarfed by thermal and apparently random air motions, but because of its characteristic period, it is possible to detect the lunar tidal component in long series of observations of certain meteorological elements. It is likely that the random element is of less importance at higher levels in the atmosphere, but at present there are no direct methods for making sustained series of observations at such altitudes. The movements of the sea and the conducting layers of the atmosphere (the ionosphere) across the Earth's main magnetic field generate electric currents, and these induce further currents in the Earth's crust and mantle. The present study is concerned with the part of the magnetic field associated with the electric currents that result from the lunar daily tides.

The lunar daily variations of the geomagnetic field,  $L$ , are very small, but have characteristic periods and remain coherent over an indefinite period of time. Thus they may be detected in a long series of observations, such as hourly mean values from magnetic observatories.

Despite its small amplitude,  $L$  is of considerable interest both in its own right, and because of the light it sheds on the intermediate processes involved in its production, e.g. the daily variation of the conductivity of the ionosphere,  $\kappa$ , the response of the atmosphere to the lunar gravitational potential, and the tidal movements of the sea. The latter are known in some detail near the coast, but very little is known of the deep sea tides. The geomagnetic lunar daily variations also form a complementary study to that of  $S$ , the solar daily geomagnetic variations, since both result from dynamo action in the ionosphere. The study of  $S$  is complicated by the coincidence of the period of the associated atmospheric oscillations (which themselves are complicated by the presence of thermal as well as gravitational components) with the period of the variation of  $\kappa$ . The period of the  $L$  variations is incommensurate with that of  $\kappa$ , and the lunar daily atmospheric oscillations are purely gravitational in origin, though it is likely that the response of the atmosphere to the gravitational potential varies with the thermal, electrical and chemical state of the atmosphere.

The main lunar tide, denoted  $M_2$ , has a period of half a lunar day, so the oscillations in the ionosphere, or oceans, may be represented by

$$a \sin (2\tau + \alpha), \quad (1)$$

where  $\tau$  denotes local lunar mean time, increasing from 0 h at one local lower transit of the mean moon to 24 h at the next;  $a$  denotes the amplitude and  $\alpha$  the phase constant of the oscillation, both dependent on geographical position. (Here, as elsewhere in this paper, where time occurs in the argument of a trigonometrical function it should be considered as an angular measure with 1 h corresponding to  $15^\circ$ , or  $\frac{1}{12}\pi$  rad.) Of the many other terms in the lunar tidal potential, all smaller than  $M_2$ , the largest would show themselves as a seasonal modulation to  $a$  and  $\alpha$ . Since

we are here concerned with the mean values of  $a$  and  $\alpha$  over a period of more than two years, the effect of such seasonal modulation may be ignored.

The conductivity of the ionosphere is controlled by the ionizing radiation from the sun, and may therefore be represented by a harmonic series in terms of  $t$ , the local mean solar time increasing from 0 h at one lower transit of the mean sun to 24 h at the next:

$$\kappa = b_0 + b_1 \sin(t + \beta_1) + b_2 \sin(2t + \beta_2) + \dots \quad (2)$$

If  $\kappa$  is proportional to the solar radiation incident on unit area of the ionosphere, its daily variation (in the mean of a year) may be represented by the positive half of a sine curve of period 24 h, with the maximum at noon. Such a curve may be very closely approximated by the first three terms of the harmonic series (see figure 1). Other curves proposed for the mean daily variation of  $\kappa$ , e.g. those of Chapman (1914) ( $1 - 3 \cos t + \frac{9}{4} \cos^2 t$ ) and Matsushita (1969) ( $[-\cos t]^{\frac{1}{2}}$  by day,  $\frac{1}{30}$  by night), may also be closely approximated by the first three terms of the harmonic series.

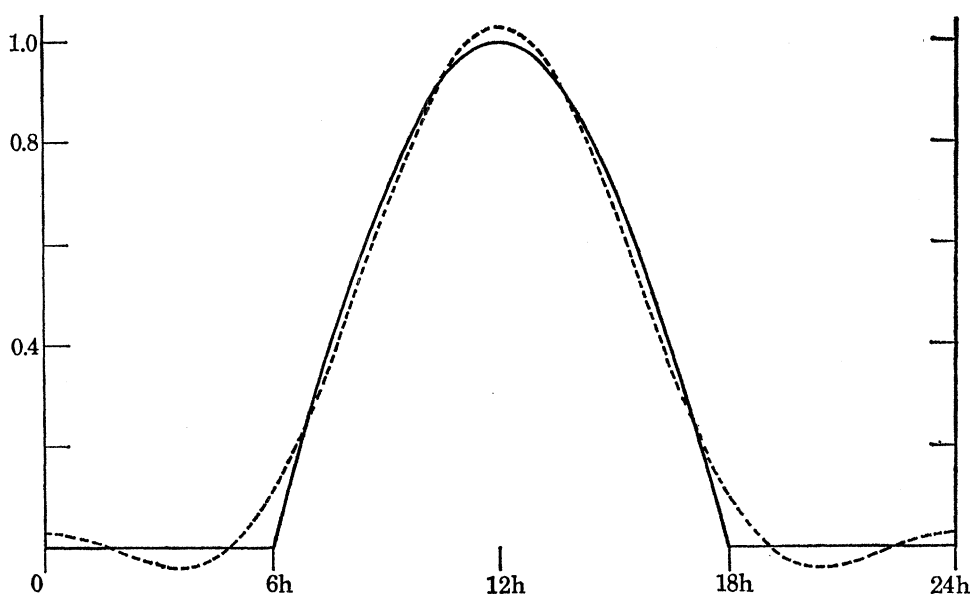


FIGURE 1. Solid curve: zero at night,  $-\cos t$  by day; broken curve: Fourier approximation.

The periodicity of magnetic variations resulting from the combined effects of the  $M_2$  tide and  $\kappa$  is indicated by the product of (1) and (2). If we truncate the series for  $\kappa$  after three terms, we obtain Chapman's phase law for  $L$ :

$$L = \sum_{n=0}^4 l_n \sin[(n-2)t + 2\tau + \lambda_n]. \quad (3)$$

Here,  $l_n$  and  $\lambda_n$  denote the amplitude and phase constant of the  $n$ th luni-solar harmonic of  $L$ . It is not generally practical to determine the  $n = 0$  term from observatory data, since it has a period of half a lunar month and is liable to be contaminated with effects due to the rotation of the Sun (Winch 1970). Also, the baseline control at most observatories is not sufficiently good to permit the reliable determination of a small variation of this period. In this study, we examine only the terms for  $n = 1, 2, 3$  and 4.

## 2. DATA AND ANALYSIS

### 2.1. *Preliminary considerations*

For a worldwide representation of  $L$ , we clearly need magnetic data with as wide a geographical coverage as possible. Since we are concerned with a small, cyclic variation, we need a sustained series of accurate observations well distributed throughout the cycle, rather than spot values. This eliminates survey data and repeat stations, leaving observatory and satellite data. The global coverage of the latter makes them particularly attractive, even though they are limited to measurements of total field, but an examination of the temporal distribution of the available satellite data shows that they are not suitable for a determination of  $L$ . The data from OGO-4 should be released shortly, and these may prove more suitable, but in view of the great difficulty experienced in extracting reliable estimates of the much larger  $S$  variations from satellite data, it is doubtful whether they can yet yield any useful information on  $L$ .

The orbits of near-Earth satellites, although external to the ionospheric dynamo layer, where the electrical currents associated with  $L$  are generated, pass among the lines of force of the main magnetic field, along which north-south currents would be expected to flow to equalize the e.m.f. at opposite ends of a line of force. Thus the satellite data are neither internal nor external to the source of  $L$ , and the interpretation of satellite  $L$  data would be extremely difficult.

For these reasons, the present study is confined to data obtained at magnetic observatories.

Previous analyses of  $L$  for single observatories (see, for example, Leaton, Malin & Finch 1962; Green & Malin 1971) have shown that there are appreciable changes of  $L$  with magnetic activity and sunspot number. Chapman, Gupta & Malin (1971) have made a detailed study of the changes with sunspot number and have shown them to be significant. For these reasons, as Matsushita & Maeda (1965*a*) have stated: 'it is certainly desirable to make a lunar analysis of the geomagnetic data obtained at many stations in different longitudinal zones during the *same* period...the method of lunar data analysis should be as dependable as possible and the same method should be applied to all the data.' Thus we require a period during which many observatories were operating simultaneously, with a broad geographical coverage. By far the best such period is the International Geophysical Year (I.G.Y., 1957.5 to 1959.0) when more observatories were operating, and with a better geographical distribution, than at any time before or since.

The 18 months of the I.G.Y. are a shorter period than is usually considered necessary for the determination of  $L$  at a non-tropical station, particularly since they occurred at sunspot maximum, when the magnetic activity was particularly high. However, Malin (1967) has shown that a realistic determination of  $L$  can be made from suitably edited I.G.Y. data from British Isles observatories. The amplitude of  $L$  increases, and the degree of disturbance decreases towards the equator, so it is reasonable to infer that, if reliable determinations can be made for the British Isles, they can also be made for stations at lower latitudes. Since this includes most of the Earth (80 % of the surface lies between latitudes  $\pm 53^\circ$ ), it appears that the I.G.Y. data are suitable for a worldwide study of  $L$ .

### 2.2. *The data*

As indicated above, the period originally selected for this study was the I.G.Y. However, after about 30 stations had been analysed, it was discovered that a similar project was being pursued at the National Center for Atmospheric Research (N.C.A.R.) by J. C. Gupta under the supervision of Professor S. Chapman. This project involved the punching of hourly values of  $D$ ,  $H$  and



$Z$ , respectively, the declination, horizontal intensity and vertical intensity of the geomagnetic field, from 100 stations for the interval 1957.5 to 1960.0 (the I.G.Y. and the subsequent International Year of Geophysical Cooperation). Clearly, there was no point in further duplication of the punching effort, and Professor Chapman kindly made the data and the computer facilities of N.C.A.R. available for the present study.

Details of the data collection, punching and editing are given by Gupta (1968). Some of the observatories closed down at the end of the I.G.Y., and for these the final year is omitted. For some observatories there are other gaps in the data, commonly on exceptionally disturbed days – which are in any case omitted from the present analysis (see §2.3) – because the trace went off the magnetogram and no supplementary insensitive records were available. The great majority of the observatories report hourly mean values, but a few report instantaneous hourly values, and these are marked for appropriate treatment in the analysis. With the exception of a few Canadian observatories where  $X$ ,  $Y$  and  $Z$  are measured ( $X$  is the north and  $Y$  the east component of the field), the original data are for the elements,  $D$ ,  $H$  and  $Z$ , but, with the exception of one observatory, these have all been converted to  $X$ ,  $Y$  and  $Z$  by Gupta, treating each hour independently. The exception is Talara ( $4.6^\circ\text{S}$ ,  $81.3^\circ\text{W}$ ), where no absolute observations of  $D$  and  $H$  have been made, so the data for this station remain as  $D$ ,  $H$  and  $Z$ .

The positions and names of the 100 observatories are indicated in figure 2.

### 2.3. Editing

The I.G.Y./I.G.C. was a period of exceptionally high magnetic activity and, with only 30 months of data, a few very disturbed days could exert an appreciable influence on the results of a lunar analysis. Thus it is important to remove at least some of the more disturbed data prior to analysis.

Malin (1967) has examined the effects of various methods of editing on  $L$  determined from I.G.Y. data in the British Isles. He concluded that the significance of the lunar harmonics, judged by the ratio of amplitude to vector probable error, may be improved by the omission of the five *International Disturbed Days* of each month. This method has the advantage of simplicity and, unlike methods based on a local measure of disturbance, leaves the same data set for each observatory.

To see if the conclusion is valid for stations at latitudes other than that of the British Isles, Chapman, Gupta & Malin (1970) analysed I.G.Y./I.G.C. data from five stations well distributed in latitude, first including all days and then omitting the *International Disturbed Days*. They found that the editing made no significant difference to the lunar amplitudes and phase angles, but that the vector probable errors were appreciably reduced. The reduction varied from a few parts per cent near the magnetic equator to over 40% at dipole latitude  $60^\circ$ . The mean reduction was 28%.

For these reasons the five *International Disturbed Days* of each month are omitted from the present analysis.

### 2.4. Method of analysis

In the past there have been many methods used to determine  $L$ , of varying degrees of sophistication, which evolved as the phenomenon of  $L$  became better understood. The two main problems are the removal of the much greater  $S$  variation, which tends to mask  $L$ , and the satisfactory treatment of errors. The method now generally used to determine  $L$  is due to Chapman & Miller (1940), who described it in conjunction with the underlying mathematical theory. The practical application of the method to a series of geophysical data was described by Tschu (1949), with a

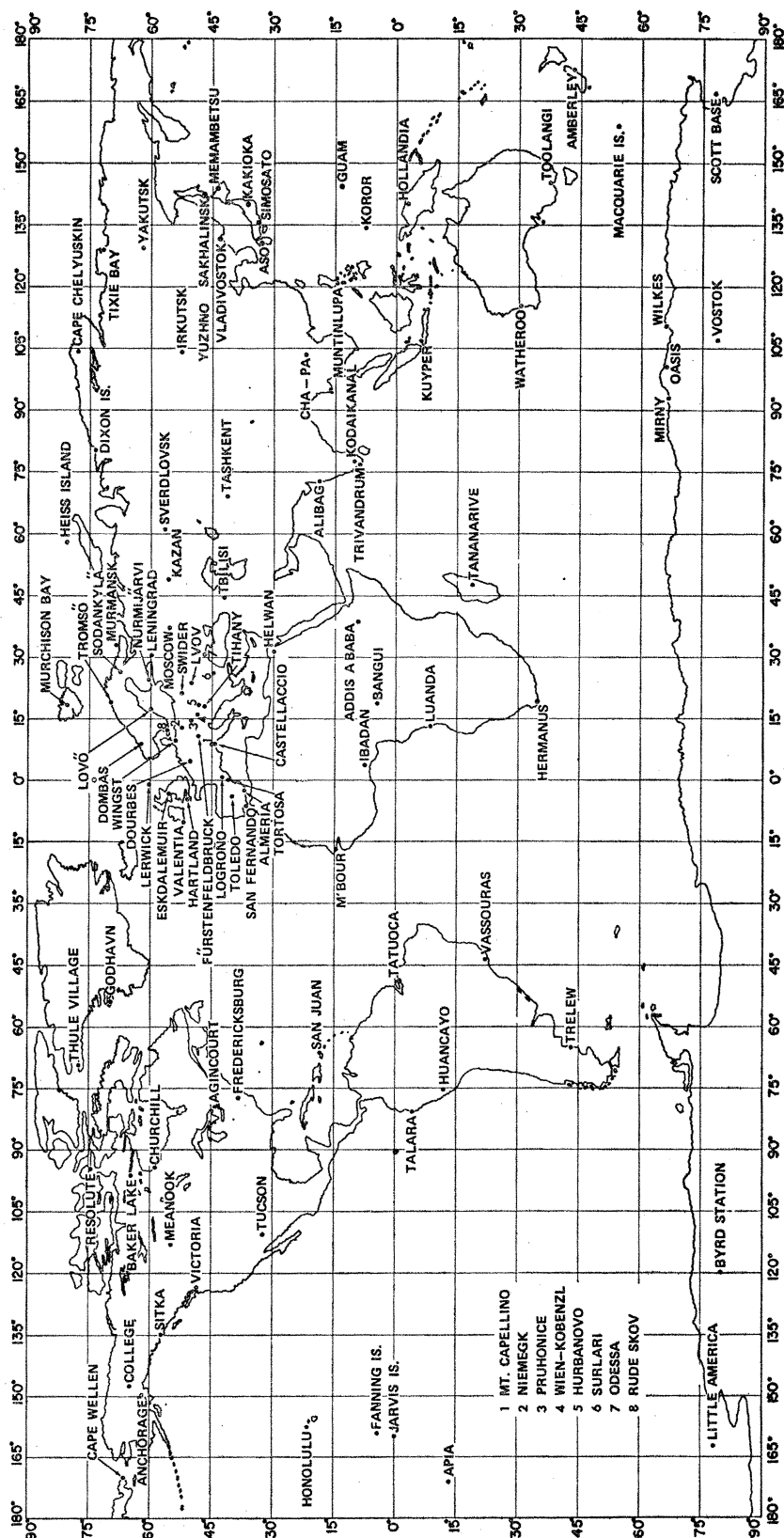


FIGURE 2. Location of observatories used in the analysis. (Reproduced by permission of J. C. Gupta.)

later correction by Chapman (1952). Leaton *et al.* (1962) have also described the practical application of the method in a form particularly suited to machine computation, and have also adapted and extended an earlier result of Miller (1934) to derive a suitable method for the determination of the vector probable errors. They also correct some minor errors in the papers by Tschu (1949) and Miller (1934). Wilkes (1962), making some simplifying assumptions, has given an elegant, but rather concentrated, mathematical derivation of the method, based on hour-to-hour differences. The primary purposes of the Chapman–Miller method of analysis is the determination of those variations that are controlled by the Moon. Variations having periods of a solar day or simple fractions of a solar day are determined as a by-product.

In response to a recommendation by the Joint I.A.G.A./I.A.M.A.P. Committee on Lunar Variations, Malin & Chapman (1970) have written an account of the Chapman–Miller method in as simple and non-mathematical a form as is compatible with rigour. This paper describes the method used here. It differs from previous methods in giving equal weight to each day in the derivation of vector probable errors as well as in the main analysis.

Power spectrum and cross spectrum techniques are becoming increasingly used in the analysis of periodic geomagnetic variations (see, for example Black 1970); however, for the study of coherent variations of known period, such as  $L$ , the Chapman–Miller method is more direct and economical in computer time than such techniques. In addition, it offers more freedom in the selection of data, and completely removes the effect of  $S$  and of non-cyclic change. Since the standard techniques of spectrum analysis can only be applied to data that is free from gaps, they are not suitable for the present data set, from which five days of each month have been omitted, in addition to numerous gaps caused by instrument failures.

### 2.5. *The analysis*

The data were analysed to determine  $l_n$ ,  $\lambda_n$  and the associated vector probable errors, for  $n = 1, 2, 3, 4$ , by the Chapman–Miller method as detailed by Malin & Chapman (1970). The vector probable error represents the radius of a circle centred on the end of the mean vector that would contain half the end-points of the observed vectors. In deriving the vector probable error, it is assumed that the 12 observed vectors are representative of a set of vectors whose end points have a two-dimensional Gaussian distribution about the mean. Although it might be more realistic to assume an elliptical distribution, it is considered that such a refinement would not be justified for so small a sample.

The  $D$  and  $H$  results for Talara have been converted to  $X$  and  $Y$  by first converting the  $D$  values from units of  $0.1'$  to nT (by multiplying each amplitude and vector probable error by  $\bar{H}/34377$ ), and then by applying the relations

$$\delta X = \delta H \cos \bar{D} - \sin \bar{D} \delta D, \quad \delta Y = \delta H \sin \bar{D} + \cos \bar{D} \delta D. \quad (4)$$

Here  $\bar{D}$  and  $\bar{H}$  denote the mean values of  $D$  and  $H$  for Talara, 1957.5 to 1959.0, synthesized from the International Geomagnetic Reference Field (Barraclough & Malin 1971);  $\delta X$  denotes a component of a lunar harmonic ( $l_n \sin \lambda_n$ , or  $l_n \cos \lambda_n$ ) for  $X$ , and  $\delta Y$ ,  $\delta H$  and  $\delta D$  denote the corresponding quantities for  $Y$ ,  $H$  and  $D$ , all expressed in nT.

For some observatories where  $D$  is measured west of north, the data for  $Y$  are positive westwards, and similarly some of the  $Z$  data are positive upwards. In these cases, the phase angles have been altered by  $180^\circ$ , so that all the results now refer to  $X$  positive northwards,  $Y$  positive eastwards and  $Z$  positive downwards.



The results of the analysis are given in tables 1 to 3 for  $X$ ,  $Y$  and  $Z$  respectively. The observatories are tabulated in decreasing order of latitude, from the north pole to the south pole. Columns 1 and 2 give the latitude and east longitude, in degrees. Column 3 gives the number of days used in each analysis; where the data are complete 764 days are available for analysis, for the I.G.Y. only there are 458 days available. The remaining four sets of three columns give for  $n = 1, 2, 3, 4$  the quantities  $l_n$  and its vector probable error in units of 0.01 nT, and  $\lambda_n$  in degrees.

As expected, the  $L$  values for the polar regions are but poorly determined, but at lower latitudes there are very many determinations where the amplitudes greatly exceed their probable errors. It should be emphasized that the errors are for vector, not scalar quantities, and a determination is significant at the 5 % level when the amplitude is 2.08 times its probable error.

TABLE 1. LUNAR HARMONICS FOR  $X$  FROM I.G.Y./I.G.C. OBSERVATORIES

The units are 0.01 nT for amplitude and p.e., degrees for latitude, longitude and phase.

lat.	long. E	no. of days	$l_1$	$\pm$	$\lambda_1$	$l_2$	$\pm$	$\lambda_2$	$l_3$	$\pm$	$\lambda_3$	$l_4$	$\pm$	$\lambda_4$
80.1	18.2	529	69	125	311	116	61	337	86	65	5	103	54	83
77.7	104.3	755	225	188	267	115	106	156	240	63	146	130	69	143
77.5	290.8	762	237	124	150	84	67	258	89	50	335	37	32	118
74.7	265.2	763	210	110	174	102	75	288	126	54	44	35	38	186
73.5	80.6	758	324	224	303	77	134	159	286	84	208	104	76	203
71.6	129.0	747	78	138	229	149	141	39	282	74	69	144	64	25
69.7	19.0	760	131	191	27	116	159	21	78	85	25	58	98	198
69.2	306.4	763	126	95	26	55	87	161	137	66	239	81	48	31
68.9	33.0	455	294	326	332	67	216	259	243	104	258	64	109	262
67.4	26.6	763	271	157	352	163	137	357	92	66	304	67	73	256
66.2	190.2	732	94	116	312	121	124	346	155	74	248	58	53	189
64.8	212.1	764	190	122	279	246	133	319	49	80	205	130	61	347
64.3	264.0	763	150	121	11	32	93	345	30	52	316	15	55	118
62.1	9.1	754	82	78	190	132	55	353	55	30	353	17	26	313
62.0	129.7	735	86	34	187	61	30	24	6	14	77	11	12	11
61.2	210.1	434	137	91	143	131	107	5	98	56	180	27	54	327
60.5	24.6	763	113	44	158	72	32	340	24	15	310	2	19	220
60.1	358.8	763	130	60	191	119	41	351	25	22	12	15	22	255
60.0	30.7	763	88	34	168	65	28	328	22	17	263	6	16	50
59.3	17.8	762	126	36	160	80	26	348	8	18	299	14	16	159
58.7	265.7	458	251	208	207	223	129	23	44	104	73	74	86	297
57.0	224.7	764	49	50	32	218	53	316	73	28	190	1	26	79
56.7	61.1	713	55	30	194	40	16	357	39	14	200	2	9	64
55.8	12.4	739	123	24	169	92	15	343	12	15	216	17	11	154
55.8	48.8	763	54	26	176	41	16	328	29	12	225	9	8	101
55.5	37.3	763	66	29	164	69	16	325	27	14	225	3	9	186
55.3	356.8	763	120	28	185	116	21	9	13	16	151	11	13	193
54.6	246.7	762	195	121	353	140	108	310	100	53	234	50	66	274
53.7	9.7	763	106	25	176	55	17	345	20	14	228	19	11	155
52.5	104.0	763	25	26	188	8	9	18	5	9	86	8	7	147
52.1	12.7	763	100	24	178	87	15	356	32	14	228	17	9	122
52.1	21.2	758	89	25	170	81	14	347	35	12	223	17	8	101
51.9	349.7	763	105	26	189	74	16	6	26	14	169	15	10	186
51.0	355.5	763	107	26	188	80	15	272	22	15	189	18	10	173
50.1	4.6	677	89	28	180	85	15	12	41	15	232	17	8	123
50.0	14.6	684	75	20	184	64	15	359	33	15	232	15	7	83
49.9	23.7	727	72	26	174	79	14	356	40	15	201	14	8	72
48.5	236.6	723	38	32	118	81	23	27	42	12	256	9	13	357
48.3	16.3	763	95	27	181	98	14	10	52	15	232	22	8	86
48.2	11.3	763	89	27	187	97	14	13	45	15	238	26	8	106
47.9	18.2	756	85	24	185	98	14	8	55	13	236	17	8	72
47.0	142.7	763	46	29	215	85	11	72	58	8	240	15	6	94

## WORLDWIDE DISTRIBUTION OF GEOMAGNETIC TIDES 559

Table 1 (*cont.*)

lat.	long. E	no. of days	$l_1$	$\pm$	$\lambda_1$	$l_2$	$\pm$	$\lambda_2$	$l_3$	$\pm$	$\lambda_3$	$l_4$	$\pm$	$\lambda_4$
46.9	17.9	763	94	26	183	102	14	14	61	16	235	25	8	86
46.8	30.9	763	81	27	175	94	14	4	59	14	219	25	8	68
44.7	26.2	752	81	31	177	93	15	6	63	15	224	31	7	64
44.5	8.9	458	81	30	177	121	19	24	67	22	248	13	16	191
44.4	8.9	757	69	29	193	124	20	15	59	15	211	25	8	41
43.9	144.2	762	43	29	234	88	12	73	61	8	240	14	7	99
43.8	280.7	763	87	40	207	70	22	34	88	16	213	29	17	12
43.1	131.9	743	62	33	238	81	17	75	43	11	252	8	7	35
42.5	0.9	705	76	38	183	189	26	21	33	21	239	37	13	129
42.1	44.7	762	75	38	176	81	17	356	62	14	205	24	9	35
41.4	69.2	763	37	35	200	17	15	34	29	11	211	16	8	2
40.8	0.5	747	63	31	207	83	18	30	42	15	251	23	8	114
39.9	355.9	763	62	29	211	66	18	37	37	14	246	20	7	122
38.2	282.6	764	71	36	196	83	14	1	68	12	161	28	11	303
36.8	357.5	719	42	35	226	82	23	36	45	17	248	21	9	94
36.5	353.8	697	65	34	218	139	25	46	55	20	282	27	14	110
36.2	140.2	763	44	27	284	103	13	85	58	8	246	12	7	112
33.6	135.9	763	38	29	310	113	13	102	52	9	251	10	7	135
32.9	131.0	745	37	28	338	71	17	122	38	11	234	4	9	351
32.2	249.2	764	13	29	281	53	18	6	45	10	180	21	11	356
29.9	31.3	749	58	44	225	87	23	67	91	13	255	35	10	83
22.4	103.8	596	72	39	22	64	17	157	21	13	273	15	13	321
21.3	201.9	764	68	26	349	56	15	14	26	8	97	21	8	291
18.6	72.9	763	100	41	10	99	19	182	29	8	348	12	9	17
18.4	293.9	764	7	23	129	76	17	42	48	8	167	18	9	310
14.4	121.0	735	149	33	23	118	14	203	46	13	60	17	9	245
14.4	343.0	761	121	25	359	115	17	205	66	11	45	24	8	252
13.4	144.7	740	199	35	6	206	16	179	83	10	21	25	7	182
10.2	77.5	610	205	38	358	265	30	187	167	23	3	44	14	178
9.0	38.7	579	295	59	26	417	39	215	308	24	37	108	16	204
8.5	76.9	534	235	43	339	308	36	182	180	19	350	45	16	118
7.3	3.9	598	267	58	25	342	31	216	238	20	36	87	15	18
7.3	134.5	458	487	81	360	569	43	194	333	44	25	81	23	212
4.4	18.5	731	145	32	4	164	18	195	120	12	20	28	9	174
3.9	200.6	411	182	47	354	127	28	166	112	21	3	32	12	201
-0.4	199.9	376	433	71	2	397	61	172	298	52	351	59	33	157
-1.2	311.5	706	133	28	2	109	19	181	53	13	17	22	10	196
-2.8	140.5	699	122	35	360	121	20	169	13	8	35	1	8	146
-4.6	278.7	458	97	41	350	118	21	150	61	14	325	39	12	64
-6.2	106.8	679	56	35	345	100	16	190	53	12	334	6	8	169
-8.8	13.2	405	55	64	336	76	31	160	50	22	18	32	17	167
-12.0	284.7	763	477	42	19	606	33	207	411	25	29	124	22	199
-13.8	188.2	719	82	26	329	218	14	106	19	9	328	6	6	307
-18.9	47.5	762	48	24	183	71	18	64	32	12	278	16	9	74
-22.4	316.3	746	89	40	358	120	20	137	48	12	271	30	7	80
-30.3	115.9	452	57	39	128	49	19	318	31	16	277	8	8	85
-34.4	19.2	763	35	24	184	67	23	57	22	16	284	34	15	22
-37.5	145.5	453	80	29	149	76	19	296	72	15	185	28	11	10
-43.2	172.7	763	66	28	148	81	14	330	43	12	140	10	8	311
-43.2	294.7	691	49	30	207	65	18	75	91	8	255	15	10	31
-54.5	158.9	304	224	237	291	284	178	331	70	119	280	188	75	238
-66.3	100.7	389	250	158	89	394	135	300	195	92	70	163	87	256
-66.4	110.4	458	148	153	49	324	148	281	188	88	39	172	74	196
-66.6	93.0	763	267	129	155	167	96	329	94	64	16	39	43	190
-77.8	166.7	455	165	148	316	190	77	285	53	67	100	4	67	154
-78.3	197.5	448	108	128	189	73	75	289	67	55	40	78	62	227
-78.4	106.9	581	110	104	76	227	66	308	84	58	109	42	40	246
-80.0	240.0	680	157	111	340	31	78	161	56	81	205	36	47	342

TABLE 2. LUNAR HARMONICS FOR  $Y$  FROM I.G.Y./I.G.C. OBSERVATORIES

The unit is 0.01 nT for amplitude and p.e., degrees for latitude, longitude and phase.

lat.	long. E	no. of days	$l_1$	$\pm$	$\lambda_1$	$l_2$	$\pm$	$\lambda_2$	$l_3$	$\pm$	$\lambda_3$	$l_4$	$\pm$	$\lambda_4$
80.1	18.2	531	53	102	172	134	59	145	91	46	9	61	37	156
77.7	104.3	755	96	60	95	155	66	12	52	40	206	39	42	36
77.5	290.8	762	167	131	104	110	86	162	37	58	311	48	57	165
74.7	265.2	763	93	129	78	69	58	204	76	53	285	59	41	79
73.5	80.6	758	99	57	96	76	43	19	54	25	295	40	36	127
71.6	129.0	747	57	51	112	103	46	322	39	36	160	31	25	161
69.7	19.0	760	100	57	125	30	49	268	24	24	134	16	22	213
69.2	306.4	763	168	90	141	15	63	272	58	55	301	40	38	129
68.9	33.0	455	142	85	95	10	53	309	14	28	11	26	23	253
67.4	26.6	763	108	60	127	53	38	271	13	20	124	30	15	215
66.2	190.2	732	58	37	100	153	30	282	3	18	88	30	20	3
64.8	212.1	764	47	61	264	208	63	259	33	47	360	97	36	317
64.3	264.0	763	64	88	47	18	58	241	51	36	266	65	39	66
62.1	9.1	754	93	40	130	62	22	288	6	11	123	15	10	227
62.0	129.7	735	58	33	92	138	32	304	28	17	141	9	12	248
61.2	210.1	434	157	59	108	188	42	254	65	30	101	42	26	274
60.5	24.6	763	85	25	122	69	18	290	27	13	136	29	6	210
60.1	358.6	763	73	44	130	79	27	255	10	15	83	21	10	239
60.0	30.7	763	89	25	121	75	17	288	39	13	129	36	7	197
59.3	17.8	762	91	29	123	71	20	287	17	13	151	25	5	221
58.7	265.7	434	122	103	174	271	78	312	26	73	94	63	56	322
57.0	224.7	764	68	33	116	220	37	261	51	22	91	34	18	268
56.7	61.1	713	80	25	89	45	18	282	32	13	42	33	8	118
55.8	12.4	739	88	28	132	85	19	276	22	12	120	20	7	221
55.8	48.8	763	69	22	98	64	18	277	41	13	78	37	7	149
55.5	37.3	763	91	24	113	86	15	284	49	12	117	31	7	171
55.3	356.8	763	67	36	141	120	20	247	14	12	67	19	8	263
54.6	246.7	762	38	63	2	245	46	270	30	33	92	36	33	300
53.7	9.7	763	79	30	137	76	17	266	15	10	110	21	7	241
52.5	104.0	763	65	26	95	120	19	301	27	11	132	19	5	38
52.1	12.7	763	89	26	139	89	16	262	23	9	127	23	6	225
52.1	21.2	758	91	23	132	79	15	282	28	8	141	23	6	203
51.9	349.7	763	47	32	134	177	20	256	26	11	77	19	7	269
51.0	355.5	763	62	31	138	203	18	246	28	10	83	12	8	275
50.1	4.6	677	94	26	150	104	20	254	18	13	71	32	7	241
50.0	14.6	684	92	28	154	71	19	261	17	10	117	16	8	237
49.9	23.7	727	108	23	141	59	16	280	27	8	146	21	5	187
48.5	236.6	723	63	18	130	201	28	292	71	12	127	21	12	294
48.3	16.3	763	90	23	138	88	17	270	32	8	122	18	6	215
48.2	11.3	763	74	26	135	97	17	259	35	9	105	17	5	237
47.9	18.2	756	89	23	130	85	16	273	36	8	119	16	5	207
47.0	142.7	763	62	18	115	125	22	304	34	14	119	7	7	124
46.9	17.9	763	88	22	138	89	15	273	36	7	121	19	5	205
46.8	30.9	763	95	20	123	95	14	288	55	8	129	19	6	183
44.7	26.2	752	87	19	132	82	14	290	47	8	136	16	6	203
44.5	8.9	458	58	33	127	98	20	258	44	16	85	10	11	332
44.4	8.9	757	73	20	129	126	16	229	50	10	70	16	9	201
43.9	144.2	762	54	20	122	114	22	306	39	13	114	6	8	139
43.8	280.7	763	45	27	52	204	29	268	51	18	107	15	11	220
43.1	131.9	743	61	22	92	140	21	299	58	12	116	10	8	284
42.5	0.9	705	67	28	132	115	18	267	49	8	74	5	8	182
42.1	44.7	762	87	22	109	101	13	288	69	9	120	16	7	136
41.4	69.2	763	53	21	107	66	13	302	24	10	116	33	8	79
40.8	0.5	747	58	31	136	132	21	273	70	11	111	25	13	231
39.9	355.9	763	74	24	130	170	16	261	64	9	104	15	8	280
38.2	282.6	764	61	18	46	205	26	234	67	15	57	17	10	186
36.8	357.5	719	70	22	126	135	18	252	72	10	90	21	7	277

Table 2 (*cont.*)

lat.	long. E	no. of days	$l_1$	$\pm$	$\lambda_1$	$l_2$	$\pm$	$\lambda_2$	$l_3$	$\pm$	$\lambda_3$	$l_4$	$\pm$	$\lambda_4$
36.5	353.8	697	72	26	123	194	24	268	76	10	99	16	8	320
36.2	140.2	763	53	21	113	145	21	299	54	12	121	9	7	351
33.6	135.9	763	51	22	107	176	20	303	73	10	124	12	7	339
32.9	131.0	745	53	25	86	132	22	317	74	14	145	15	8	6
32.2	249.2	764	52	19	89	170	17	251	96	11	70	33	7	237
29.9	31.3	749	78	21	128	84	15	298	70	9	150	12	9	353
22.4	103.8	596	48	28	174	109	24	352	55	17	175	14	9	7
21.3	201.9	764	34	16	130	139	16	258	79	13	80	28	6	250
18.6	72.9	763	45	26	146	79	18	340	38	10	148	8	7	220
18.4	293.9	764	67	20	19	232	22	229	117	11	53	40	5	241
14.4	121.0	735	40	19	71	127	13	300	69	10	135	12	7	18
14.4	343.0	761	84	19	135	113	16	280	100	10	130	35	8	350
13.4	144.7	740	49	24	147	134	17	322	69	10	155	14	10	13
10.2	77.5	610	67	22	180	83	20	31	43	12	205	23	8	17
9.0	38.7	579	66	26	246	33	27	102	26	15	105	38	8	299
8.5	76.9	534	16	21	163	32	18	359	5	12	126	8	7	120
7.3	3.9	598	31	27	88	53	22	239	18	12	221	32	8	82
7.3	134.5	458	63	25	153	106	20	334	49	14	177	13	8	47
4.4	18.5	731	19	25	62	65	18	138	53	10	286	29	7	86
3.9	200.6	411	45	24	244	25	22	300	29	13	104	31	6	264
-0.4	199.9	376	54	26	290	30	23	120	14	14	339	21	9	258
-1.2	311.5	706	55	23	164	97	22	246	91	11	72	35	7	255
-2.8	140.5	699	52	39	246	73	24	29	60	16	252	37	10	95
-4.6	278.7	458	269	59	348	299	43	206	236	27	53	91	19	236
-6.2	106.8	679	92	28	44	122	17	239	73	9	76	35	5	283
-8.8	13.2	405	84	33	229	109	24	111	55	17	301	35	9	129
-12.0	284.7	763	191	25	9	218	15	206	113	9	44	23	7	239
-13.8	188.2	719	105	21	260	133	15	68	79	14	260	12	6	61
-18.9	47.5	762	28	25	324	174	20	131	70	15	276	22	8	67
-22.4	316.3	746	13	20	313	120	18	140	117	10	286	52	7	58
-30.3	115.9	452	73	27	185	135	21	61	93	13	256	15	9	72
-34.4	19.2	763	24	26	256	124	19	109	53	14	258	27	9	71
-37.5	145.5	453	78	31	237	171	29	51	69	17	226	7	9	69
-43.2	172.7	763	68	28	254	191	17	38	37	10	202	17	10	16
-43.2	294.7	691	75	21	304	154	19	146	75	12	296	23	8	92
-54.5	158.9	304	148	105	286	263	80	10	37	50	259	88	34	217
-66.3	100.7	389	263	172	337	169	120	190	104	87	239	65	65	58
-66.4	110.4	458	88	162	13	68	145	231	87	80	224	59	72	77
-66.6	93.0	763	238	108	277	228	80	40	66	60	151	78	37	31
-77.8	166.7	455	345	105	99	147	100	330	81	72	78	13	52	89
-78.3	197.5	448	300	147	189	44	92	42	123	91	97	43	62	258
-78.4	106.9	581	320	117	194	114	67	27	61	59	197	135	45	22
-80.0	240.0	680	248	127	281	200	100	294	28	85	323	36	52	300

In general, the  $n = 2$  terms have the largest amplitude, again as expected, but these show more erratic changes with geographical position than do the other harmonics. The reason for this is considered in §3.

### 3. DETERMINATION AND REMOVAL OF THE OCEAN DYNAMO EFFECT

#### 3.1. *The method*

The lunar harmonics determined in §2.5 contain contributions from both the ionospheric and the oceanic dynamos. The ocean dynamo effect results from tidal movements of the sea across the Earth's main magnetic field. Since the conductivity of the sea has negligible time

TABLE 3. LUNAR HARMONICS FOR  $Z$  FROM I.G.Y./I.G.C. OBSERVATORIES

The unit is 0.01 nT for amplitude and p.e., degrees for latitude, longitude and phase.

lat.	long. E	no. of days	$l_1$	$\pm$	$\lambda_1$	$l_2$	$\pm$	$\lambda_2$	$l_3$	$\pm$	$\lambda_3$	$l_4$	$\pm$	$\lambda_4$
80.1	18.2	527	40	164	104	107	86	168	71	54	127	153	39	234
77.7	104.3	762	257	182	108	95	111	87	258	65	332	78	57	309
77.5	290.8	761	112	124	157	85	76	259	38	53	92	10	42	91
74.7	265.2	745	286	191	167	81	85	264	75	51	71	53	40	226
73.5	80.6	761	130	86	128	111	86	152	50	60	309	64	49	312
71.6	129.0	747	17	106	227	29	57	202	49	33	317	34	36	148
69.7	19.0	760	219	108	162	139	106	276	124	53	75	67	66	79
69.2	306.4	763	100	106	58	239	76	167	97	60	354	69	50	223
68.9	33.0	445	192	83	167	82	91	236	87	61	64	82	57	90
67.4	26.6	763	32	107	30	17	49	143	35	51	71	19	51	142
66.2	190.2	760	142	76	254	66	45	313	51	41	172	70	40	108
64.8	212.1	764	93	77	204	47	61	8	100	52	24	69	54	343
64.3	264.0	754	158	117	96	234	69	155	166	65	336	94	43	75
62.1	9.1	755	125	82	358	101	54	5	35	32	10	44	26	311
62.0	129.7	457	27	49	221	67	25	323	27	19	331	9	15	44
61.2	210.1	434	105	77	194	62	78	165	82	38	73	69	34	338
60.5	24.6	763	74	47	321	36	40	340	27	18	313	34	20	243
60.1	358.8	763	71	76	20	271	60	358	46	26	26	16	24	336
60.0	30.7	686	5	43	270	8	32	339	43	19	331	13	17	236
59.3	17.8	763	40	43	312	19	34	348	19	16	338	30	16	262
58.7	265.7	423	156	187	86	132	109	88	126	109	83	81	85	94
57.0	224.7	764	108	68	292	100	51	302	63	39	209	18	24	260
56.7	61.1	763	31	26	318	34	13	8	17	7	216	9	7	191
55.8	12.4	763	8	28	165	24	21	259	11	11	21	22	10	257
55.8	48.8	762	19	19	306	24	15	45	18	7	269	12	6	213
55.5	37.3	763	20	22	310	9	18	67	16	6	340	17	7	211
55.3	356.8	763	35	30	165	68	26	30	6	11	17	19	9	312
54.6	246.7	761	205	98	305	167	54	322	40	37	259	57	33	341
53.7	9.7	763	17	24	135	42	17	250	15	9	71	15	8	254
52.5	104.0	763	14	10	144	26	8	343	7	6	122	10	5	126
52.1	12.7	763	19	20	101	54	13	337	13	6	83	12	6	236
52.1	21.2	409	28	30	135	40	19	340	6	10	207	19	10	195
51.9	349.7	763	48	24	183	287	18	11	18	10	126	19	7	312
51.0	355.5	763	46	20	168	239	14	354	20	7	123	9	6	281
50.1	4.6	682	12	18	114	61	12	335	18	7	127	9	5	223
50.0	14.6	721	24	21	55	43	12	308	17	7	71	9	6	213
49.9	23.7	723	18	20	20	22	10	283	8	8	105	13	5	238
48.5	236.6	721	21	23	248	39	17	115	18	15	227	3	10	64
48.3	16.3	763	24	16	79	43	10	317	11	6	86	10	5	217
48.2	11.3	759	26	17	125	54	11	319	16	6	116	12	4	218
47.9	18.2	760	27	14	76	40	8	304	14	5	108	11	4	221
47.0	142.7	763	40	10	152	37	6	330	7	4	237	2	2	253
46.9	17.9	763	25	14	80	41	8	303	15	6	111	7	4	210
46.8	30.9	763	24	14	33	23	7	277	12	4	57	10	4	193
44.7	26.2	753	25	16	72	40	7	293	14	5	105	8	4	198
44.5	8.9	458	18	23	133	49	10	308	8	8	108	6	4	231
43.9	144.2	761	45	9	153	47	5	312	14	3	258	4	2	131
43.8	280.7	763	42	35	289	77	31	285	26	14	216	18	11	135
43.1	131.9	730	26	13	132	30	9	311	6	6	225	4	4	46
42.5	0.9	673	39	14	146	51	10	281	24	6	110	8	5	258
42.1	44.7	762	31	12	37	31	8	276	14	5	89	7	4	206
41.4	69.2	763	39	10	203	41	6	6	23	4	190	8	4	160
40.8	0.5	746	30	12	172	117	12	3	16	5	142	8	5	223
39.9	355.9	763	42	9	167	83	8	345	28	4	138	4	3	267
38.2	282.6	764	23	19	204	44	16	260	25	8	138	2	3	100
36.8	357.5	719	36	11	185	149	10	38	17	7	133	7	4	146
36.2	140.2	762	35	12	159	32	7	280	38	6	266	11	4	143



Table 3 (*cont.*)

lat.	long. E	no. of days	$l_1$	$\pm$	$\lambda_1$	$l_2$	$\pm$	$\lambda_2$	$l_3$	$\pm$	$\lambda_3$	$l_4$	$\pm$	$\lambda_4$
33.6	135.9	763	36	16	173	100	9	182	50	8	283	13	6	166
32.9	131.0	744	56	12	173	52	7	29	34	6	230	6	4	92
32.2	249.2	764	29	13	115	24	9	1	27	6	121	5	4	292
29.9	31.3	756	59	9	171	91	9	349	60	6	167	20	5	338
22.4	103.8	612	31	11	302	5	7	38	4	5	278	4	4	238
21.3	201.9	764	27	11	114	33	10	95	36	8	121	17	5	299
18.6	72.9	763	54	18	210	51	14	45	71	7	211	12	6	41
18.4	293.9	764	37	10	145	70	8	271	31	4	132	14	3	315
14.4	121.0	737	100	14	186	173	11	16	99	13	211	27	10	63
14.4	343.0	761	95	13	210	175	14	39	117	11	208	44	10	55
13.4	144.7	741	101	16	188	144	9	350	53	6	185	9	3	28
10.2	77.5	610	47	16	115	26	14	316	28	12	152	11	7	61
9.0	38.7	592	24	13	260	47	10	51	35	5	237	14	5	25
8.5	76.9	534	89	21	7	151	18	180	85	14	3	35	10	130
7.3	3.9	613	173	22	195	218	21	26	185	17	208	61	11	23
7.3	134.5	458	59	27	29	151	15	262	102	16	71	31	10	258
4.4	18.5	730	68	15	182	122	12	3	96	8	170	43	5	342
3.9	200.6	333	130	35	178	94	22	349	73	18	145	20	12	310
-0.4	199.9	338	23	9	77	74	14	222	26	9	50	16	7	245
-1.2	311.5	704	91	19	249	140	14	124	123	8	343	39	6	209
-2.8	140.5	695	75	19	326	68	15	129	52	10	350	26	6	173
-4.6	278.7	458	82	35	139	225	28	357	211	24	143	87	15	315
-6.2	106.8	680	38	17	18	18	11	20	39	7	339	13	4	167
-8.8	13.2	376	100	49	12	137	29	199	115	22	27	37	15	187
-12.0	284.7	763	116	12	152	141	10	343	86	7	161	24	5	344
-13.8	188.2	722	41	11	302	161	5	132	7	4	15	1	2	23
-18.9	47.5	763	36	13	353	153	8	170	7	5	292	4	3	94
-22.4	316.3	740	83	15	354	83	10	190	73	7	350	26	5	137
-30.3	115.9	453	76	25	231	307	20	62	113	12	288	37	9	123
-34.4	19.2	763	33	16	351	110	20	205	45	11	330	29	7	95
-37.5	145.5	451	16	31	206	61	13	55	23	9	235	10	6	45
-43.2	172.7	763	23	17	142	292	9	54	17	5	223	3	3	350
-43.2	294.7	688	69	13	38	57	8	178	49	6	340	17	6	138
-54.5	158.9	304	242	85	43	469	114	349	185	61	49	51	63	79
-66.3	100.7	392	224	152	108	17	134	337	122	97	156	95	69	64
-66.4	110.4	458	394	187	120	178	135	308	85	104	108	26	101	292
-66.6	93.0	763	158	97	310	367	92	133	132	78	268	96	64	98
-77.8	166.7	446	141	106	209	83	66	180	75	63	132	8	42	276
-78.3	197.5	448	354	167	241	44	122	355	92	64	159	78	59	65
-78.4	106.9	573	222	116	301	121	67	103	70	51	183	56	34	249
-80.0	240.0	681	392	179	293	215	73	0	48	56	101	30	54	186

dependence, the dynamo currents resulting from the  $M_2$  ocean tide depend only on lunar time, and contribute only to the  $n = 2$  term in equation (3).

Malin (1970) has shown how, making reasonable assumptions, the  $n = 2$  term may be separated into parts of oceanic,  $L_O$ , and ionospheric,  $L_I$ , origin. The main assumption is that the ionospheric conductivity, and hence the ionospheric contribution to  $L$ , becomes negligibly small at local midnight, but  $L_O$  is undiminished. Then, if the ionospheric contribution is adequately represented by four harmonics:

$$\left. \begin{aligned} l_O \sin \lambda_O &= \sum_{n=1}^4 l_n \sin \lambda_n, \\ l_O \cos \lambda_O &= \sum_{n=1}^4 l_n \cos \lambda_n, \\ \rho_O &= \left[ \sum_{n=1}^4 (\rho_n)^2 \right]^{\frac{1}{2}}, \end{aligned} \right\} \quad (5)$$

$$\left. \begin{aligned} l_1 \sin \lambda_1 &= -l_1 \sin \lambda_1 - l_3 \sin \lambda_3 - l_4 \sin \lambda_4, \\ l_1 \cos \lambda_1 &= -l_1 \cos \lambda_1 - l_3 \cos \lambda_3 - l_4 \cos \lambda_4, \end{aligned} \right\} \quad (6)$$

and

$$\rho_1 = [(\rho_1)^2 + (\rho_2)^2 + (\rho_3)^2]^{\frac{1}{2}};$$

where

$$L_0 = l_0 \sin (2\tau + \lambda_0), \quad (7)$$

$$L_1 = l_1 \sin (2\tau + \lambda_1), \quad (8)$$

$\rho_n$  denotes the vector probable error of the  $n$ th luni-solar harmonic of  $L$ , and  $\rho_1$  and  $\rho_0$  denote the vector probable errors of  $L_1$  and  $L_0$ .

The method was applied to six observatories in the British Isles, and Chapman & Kendall (1970) showed the determinations of  $L_0$  to be in fair agreement with those that they calculated from a theoretical model based on linear channels representing, in idealized form, the North Sea, English Channel, Irish Sea and Atlantic Ocean. This agreement with theory and the fact that  $L_0$  is of insignificant amplitude for far inland stations, e.g. Irkutsk (Malin 1970) and Hyderabad (Sastri & Rao 1971), give confidence in the method of determining  $L_0$ . Furthermore, the  $L_1$  vectors showed a much more consistent pattern over the British Isles than did the original  $L_2$  vectors, indicating the importance of removing the ocean effect prior to any analysis of the ionospheric effect.

It is interesting to note that the ionospheric dynamo effect is independent of the observed values of  $l_2$  and  $\lambda_2$  (see equations (6)), although  $L_1$  reduces to  $L_2$  when the ocean effect is small. This must cast doubt on the validity of ionospheric current systems deduced from studies of  $L_2$  data alone.

### 3.2. Application to worldwide observatories

The methods of §3.1 have already been applied to a number of individual stations. In addition to those already mentioned, ocean effects have been determined for Alibag, Annamalainagar, Kodaikanal & Trivandrum by Sastri & Rao (1971), Watheroo (Green & Malin 1971), Toolangi (Green 1972) and Stonyhurst (J. E. Worthy, private communication). Here, we apply the method to the data for 100 I.G.Y./I.G.C. stations given in tables 1 to 3. The resulting components of  $L_2$  are given in tables 4 (ionospheric part) and 5 (oceanic part). The first two columns of these tables correspond with columns 1 and 2 of tables 1 to 3. The remaining three sets of three columns give, for  $X$ ,  $Y$  and  $Z$ , the amplitude ( $l_1$  or  $l_0$ ) and its vector probable error in units of 0.01 nT, and the phase constant ( $\lambda_1$  or  $\lambda_0$ ) in degrees. Vector addition of the corresponding entries in tables 4 and 5 reproduces the values of  $l_2$  and  $\lambda_2$  given in tables 1 to 3.

As was found for the British Isles, the  $L_1$  vectors are noticeably more ordered than the  $L_2$  vectors. The  $L_0$  vectors show considerable scatter, but, as expected, show a tendency to be greater near the coast than inland. However, Chapman & Kendall (1970) have shown that the ocean effect is an extremely complex phenomenon, depending as much on tides in the distant, deep oceans as on those in nearby, shallow channels. For a satisfactory model of the ocean effect, it is necessary to take account of the worldwide distribution of ocean tides and ocean depths. Professor P. C. Kendall and Dr R. Hewson-Browne of the University of Sheffield are working on such a model, using the tidal model of Pekeris & Accad (1969). To predict the ocean effect at a specific site, the model will probably have to be modified to take account of local features, such as estuaries and bays. The test of the quality of the model will be the accuracy with which it can reproduce the data given in table 5. It is hoped that differences between the predicted and observed ocean effects will indicate areas where the model is weak, and hence lead to a better knowledge of the pelagic tides.

## WORLDWIDE DISTRIBUTION OF GEOMAGNETIC TIDES 565

TABLE 4. IONOSPHERIC PART OF  $L_2$  FOR  $X$ ,  $Y$  AND  $Z$  FROM I.G.Y./I.G.C. OBSERVATORIES

Unit = 0.01 nT

lat.	long. E	$X$ ,			$Y$ ,			$Z$ ,		
		$l_I$	$\pm$	$\lambda_I$	$l_I$	$\pm$	$\lambda_I$	$l_I$	$\pm$	$\lambda_I$
80.1°	18.2°	154	151	202°	50	118	291°	145	177	11°
77.7	104.3	316	210	2	99	83	283	207	201	198
77.5	290.8	182	137	321	159	154	293	139	141	319
74.7	265.2	188	128	325	90	145	237	308	202	342
73.5	80.6	479	251	69	82	72	278	17	116	288
71.6	129.0	321	169	236	116	67	319	28	117	81
69.7	19.0	152	231	209	126	66	314	301	137	303
69.2	306.4	113	125	170	153	112	326	103	132	195
68.9	33.0	483	359	115	119	92	274	252	118	306
67.4	26.6	352	185	150	125	65	320	65	129	248
66.2	190.2	229	147	77	65	46	252	128	95	29
64.8	212.1	262	158	115	150	85	131	74	107	167
64.3	264.0	163	143	188	87	103	219	240	141	228
62.1	9.1	36	88	66	98	43	319	191	92	171
62.0	129.7	73	39	2	73	39	292	26	55	111
61.2	210.1	197	120	340	181	71	289	31	92	296
60.5	24.6	94	50	346	118	29	320	114	54	122
60.1	358.8	112	68	18	74	48	320	128	84	197
60.0	30.7	85	41	0	142	29	317	48	50	129
59.3	17.8	134	43	342	108	32	321	78	49	121
58.7	265.7	225	248	38	73	138	359	362	233	267
57.0	224.7	33	63	334	84	44	292	149	82	83
56.7	61.1	93	34	15	131	29	266	33	28	91
55.8	12.4	148	30	351	111	31	320	16	32	81
55.8	48.8	77	30	6	132	26	284	40	21	91
55.5	37.3	86	33	1	159	28	304	32	24	114
55.3	356.8	142	35	3	61	39	324	16	33	12
54.6	246.7	207	148	132	55	78	180	279	110	126
53.7	9.7	136	31	0	88	32	326	16	27	313
52.5	104.0	32	28	349	97	29	275	31	13	313
52.1	12.7	131	29	3	114	28	328	23	22	292
52.1	21.2	117	29	356	129	25	324	45	33	345
51.9	349.7	145	31	5	48	35	304	46	27	3
51.0	355.5	146	32	6	71	34	306	57	22	342
50.1	4.6	125	33	9	98	30	339	29	20	319
50.0	14.6	95	26	10	108	31	337	33	23	249
49.9	23.7	105	31	357	151	25	328	8	22	200
48.5	236.6	21	37	21	114	25	311	35	29	58
48.3	16.3	127	32	9	125	25	322	29	18	275
48.2	11.3	122	32	11	101	28	315	42	18	318
47.9	18.2	116	28	18	128	25	314	33	15	280
47.0	142.7	92	31	42	103	24	297	41	11	345
46.9	17.9	130	32	13	130	24	321	36	16	281
46.8	30.9	118	31	4	161	22	311	27	15	231
44.7	26.2	113	35	6	140	21	319	35	17	276
44.5	8.9	133	40	27	88	38	285	25	25	319
44.4	8.9	103	34	17	107	24	294			
43.9	144.2	94	31	52	98	25	300	47	10	348
43.8	280.7	147	46	33	75	34	269	47	39	64
43.1	131.9	97	35	66	106	26	284	26	15	316
42.5	0.9	116	45	2	103	30	291	56	16	319
42.1	44.7	111	41	4	170	25	296	35	14	237
41.4	69.2	51	38	32	106	25	281	68	11	14
40.8	0.5	92	35	31	119	35	314	49	14	350
39.9	355.9	93	33	32	120	27	300	67	10	339
38.2	282.6	119	40	10	116	25	238	41	21	347

Table 4 (*cont.*)

lat.	long. E	$X_s$			$Y_s$			$Z_s$		
		$l_1$	$\pm$	$\lambda_1$	$l_1$	$\pm$	$\lambda_1$	$l_1$	$\pm$	$\lambda_1$
36.8°	357.5°	70	40	47°	115	25	290°	55	14	346°
36.5	353.8	84	42	55	131	29	287			
36.2	140.2	86	29	78	102	25	293	48	14	23
33.6	135.9	71	31	90	114	25	293	55	19	48
32.9	131.0	48	31	109	105	30	293	79	14	10
32.2	249.2	26	33	34	115	23	262	51	15	298
29.9	31.3	112	47	58	136	25	315	99	12	351
22.4	103.8	79	43	178	89	34	353	37	13	114
21.3	201.9	72	28	174	80	21	283	46	14	297
18.6	72.9	139	43	186	86	29	332	113	20	29
18.4	293.9	40	26	356	140	23	215	54	11	320
14.4	121.0	174	37	208	94	23	285	176	22	12
14.4	343.0	162	28	188	158	23	305	174	20	22
13.4	144.7	255	37	191	108	28	327	146	17	6
10.2	77.5	328	47	181	85	26	8	76	21	301
9.0	38.7	494	66	213	70	31	77	48	15	77
8.5	76.9	383	50	169	27	25	325	156	27	196
7.3	3.9	417	63	209	52	31	279	295	30	22
7.3	134.5	727	95	188	104	30	337	123	33	230
4.4	18.5	236	35	193	26	28	168	122	18	0
3.9	200.6	264	53	174	53	28	55	180	41	350
-0.4	199.9	673	94	180	81	31	109	32	15	241
-1.2	311.5	163	32	185	77	26	297	150	21	110
-2.8	140.5	132	37	183	80	43	57	100	22	151
-4.6	278.7	164	45	174	357	68	189	207	45	325
-6.2	106.8	103	38	159	136	30	227	60	19	181
-8.8	13.2	67	70	181	97	38	60	177	56	203
-12.0	284.7	761	54	204	273	27	199	178	15	335
-13.8	188.2	107	28	147	173	26	82	44	12	132
-18.9	47.5	43	28	25	77	30	120	39	14	170
-22.4	316.3	97	42	167	104	23	131	135	17	178
-30.3	115.9	38	43	324	123	31	42	139	29	77
-34.4	19.2	11	33	100	50	31	81	69	21	181
-37.5	145.5	119	34	340	140	36	51	28	33	42
-43.2	172.7	99	31	326	83	31	64	28	18	356
-43.2	294.7	116	33	62	130	25	124	95	16	203
-54.5	158.9	438	276	89	235	121	81	470	122	229
-66.3	100.7	277	202	264	261	203	149	375	193	292
-66.4	110.4	199	191	247	40	194	205	452	237	298
-66.6	93.0	231	150	325	169	129	103	178	140	118
-77.8	166.7	123	176	151	435	138	275	174	130	7
-78.3	197.5	113	152	16	322	184	354	306	188	42
-78.4	106.9	149	126	277	248	139	10	247	131	96
-80.0	240.0	159	145	145	304	161	107	337	195	110

4. WORLDWIDE REPRESENTATION OF THE IONOSPHERIC PART OF  $L$ 4.1. *Choice of method*

There have been two main methods proposed for the analysis and interpolation of geomagnetic variation fields. These are: spherical harmonic analysis (Gauss 1839), and the surface integral method (Hasegawa 1936; Vestine 1941). Both methods have been considerably refined since their introduction, and we here discuss the surface integral method in the version of Price & Wilkins (1963).

## WORLDWIDE DISTRIBUTION OF GEOMAGNETIC TIDES 567

TABLE 5. OCEANIC PART OF  $L_2$  FOR  $X$ ,  $Y$  AND  $Z$  FROM I.G.Y./I.G.C. OBSERVATORIES

lat.	long. E	Unit = 0.01 nT								
		$X$ ,			$Y$ ,			$Z$ ,		
		$l_0$	$\pm$	$\lambda_0$	$l_0$	$\pm$	$\lambda_0$	$l_0$	$\pm$	$\lambda_0$
80.1°	18.2°	249	163	3°	178	132	136°	247	197	181°
77.7	104.3	422	235	175	182	106	45	256	230	38
77.5	290.8	161	153	168	246	177	133	121	160	176
74.7	265.2	122	149	175	50	157	106	300	219	177
73.5	80.6	487	285	239	122	84	60	124	144	146
71.6	129.0	466	220	51	14	81	114	49	130	231
69.7	19.0	267	280	26	107	82	145	188	173	143
69.2	306.4	60	152	357	145	129	150	157	152	149
68.9	33.0	539	419	290	111	107	91	237	149	145
67.4	26.6	502	230	338	99	75	164	72	138	81
66.2	190.2	261	193	284	102	55	300	129	105	239
64.8	212.1	497	207	306	323	106	281	119	124	355
64.3	264.0	193	170	4	70	118	34	283	157	101
62.1	9.1	126	103	337	55	48	174	289	106	356
62.0	129.7	28	49	128	69	50	317	90	60	314
61.2	210.1	96	161	124	110	83	185	86	121	149
60.5	24.6	23	60	184	67	34	170	144	67	311
60.1	358.8	54	79	281	82	55	200	394	103	4
60.0	30.7	45	50	229	85	34	163	55	59	313
59.3	17.8	55	51	154	63	38	180	92	59	310
58.7	265.7	59	279	299	228	159	298	494	257	87
57.0	224.7	187	82	312	155	57	244	236	97	279
56.7	61.1	56	38	208	89	34	78	44	31	321
55.8	12.4	58	34	183	77	37	190	40	38	259
55.8	48.8	51	34	216	69	32	111	29	26	308
55.5	37.3	51	37	235	84	32	145	27	30	308
55.3	356.8	29	41	159	121	44	218	53	42	35
54.6	246.7	347	183	311	252	91	283	442	122	312
53.7	9.7	85	35	190	82	37	199	38	32	227
52.5	104.0	25	30	161	53	34	353	15	15	75
52.1	12.7	45	33	195	112	32	194	41	25	1
52.1	21.2	39	32	195	88	29	181	6	38	197
51.9	349.7	71	35	185	149	40	241	242	32	12
51.0	355.5	172	35	214	180	38	225	184	26	358
50.1	4.6	41	36	180	136	36	208	34	23	349
50.0	14.6	35	30	213	114	36	194	38	26	356
49.9	23.7	26	34	179	119	30	169	23	24	304
48.5	236.6	60	43	29	100	37	271	36	34	171
48.3	16.3	29	35	185	99	30	186	29	20	359
48.2	11.3	25	35	182	93	33	195	12	21	325
47.9	18.2	26	32	241	84	30	175	17	17	357
47.0	142.7	46	33	155	26	32	332	11	12	224
46.9	17.9	28	35	191	98	28	184	15	18	3
46.8	30.9	24	34	183	83	26	158	20	17	355
44.7	26.2	20	38	188	80	26	170	12	19	350
44.5	8.9	14	45	234	44	43	194	25	27	298
44.4	8.9	21	39	5	125	29	179	—	—	—
43.9	144.2	34	33	162	20	33	342	29	11	240
43.8	280.7	77	51	212	129	45	267	117	50	270
43.1	131.9	21	39	209	46	34	335	5	17	279
42.5	0.9	88	52	46	47	35	203	35	19	202
42.1	44.7	33	45	204	71	28	126	22	16	356
41.4	69.2	34	40	211	51	28	72	28	13	205
40.8	0.5	9	40	213	89	41	211	70	18	11
39.9	355.9	28	38	198	109	31	216	18	13	8
38.2	282.6	39	42	209	89	36	229	59	26	215
36.8	357.5	19	46	352	82	31	195	123	17	58



Table 5 (*cont.*)

lat.	long. E	$X,$			$Y,$			$Z,$		
		$l_0$	$\pm$	$\lambda_0$	$l_0$	$\pm$	$\lambda_0$	$l_0$	$\pm$	$\lambda_0$
36.5°	353.8°	57	49	33°	82	38	236°	—		
36.2	140.2	19	32	112	45	33	312	63	16	232°
33.6	135.9	46	34	119	66	32	320	144	21	198
32.9	131.0	26	36	146	55	37	7	34	16	160
32.2	249.2	32	37	344	61	29	229	46	17	90
29.9	31.3	30	52	209	61	29	160	9	15	195
22.4	103.8	30	46	47	20	42	349	36	15	302
21.3	201.9	126	32	3	76	27	230	77	18	108
18.6	72.9	41	47	16	13	34	96	65	25	197
18.4	293.9	56	31	73	103	32	249	54	14	221
14.4	121.0	58	39	40	45	26	335	10	24	122
14.4	343.0	63	33	334	72	28	165	50	24	119
13.4	144.7	69	40	50	28	33	302	41	20	266
10.2	77.5	71	55	335	34	33	112	52	25	113
9.0	38.7	77	76	27	43	41	239	21	18	331
8.5	76.9	110	61	308	18	31	57	43	33	90
7.3	3.9	89	70	0	36	38	171	79	37	189
7.3	134.5	176	104	345	5	36	263	80	36	317
4.4	18.5	72	40	10	45	33	121	7	21	89
3.9	200.6	140	60	2	67	36	255	86	47	171
−0.4	199.9	285	112	11	52	38	283	45	20	209
−1.2	311.5	55	38	12	76	34	196	37	26	223
−2.8	140.5	33	42	67	38	50	303	45	27	6
−4.6	278.7	74	50	35	110	80	319	121	53	62
−6.2	106.8	55	41	267	30	34	351	77	22	5
−8.8	13.2	27	76	100	89	45	168	41	63	35
−12.0	284.7	158	63	15	63	31	353	43	18	127
−13.8	188.2	154	31	79	53	30	296	117	13	132
−18.9	47.5	46	34	100	100	36	140	114	16	171
−22.4	316.3	62	47	83	24	30	182	57	20	341
−30.3	115.9	12	47	297	44	38	126	176	35	51
−34.4	19.2	59	40	50	83	36	126	55	29	236
−37.5	145.5	84	39	199	31	47	50	34	35	65
−43.2	172.7	19	34	129	122	36	20	278	20	58
−43.2	294.7	54	37	226	59	32	201	50	17	52
−54.5	158.9	622	328	293	290	145	320	813	167	19
−66.3	100.7	235	243	343	174	236	289	364	235	110
−66.4	110.4	193	242	316	36	243	259	278	272	111
−66.6	93.0	65	178	136	216	152	355	200	167	146
−77.8	166.7	289	192	303	372	170	76	256	146	185
−78.3	197.5	131	170	230	295	205	167	278	224	229
−78.4	106.9	126	142	346	143	154	176	127	147	270
−80.0	240.0	129	165	322	503	190	290	457	208	316

The Price–Wilkins method proceeds as follows:

(i) Obtain observatory data for the geomagnetic variations in  $X$ ,  $Y$ , and  $Z$  for a selection of epochs of U.T. distributed throughout the cycle of the variation.

(ii) For each selected epoch, interpolate values of  $X$ ,  $Y$  and  $Z$  at the points of intersection of a set of geographical meridians and latitude circles. For this interpolation, it is assumed that the variations in the vicinity of an observatory pass along a locus through the observatory at the same rate as the Sun ( $15^\circ$  W per hour) without changing in amplitude or phase. These loci are determined from a subjective examination of the observatory data, and broadly follow lines of equal dip.

(iii) The grid-point values of  $X$  and  $Y$  are adjusted by a relaxation method until they represent a potential field. For such a field, the integral of potential around a closed contour is zero.

The potential difference between grid-points is proportional to the product of the separation of the points and (*a*) the difference in the values of  $Y$  for points at the same latitude, or (*b*) the difference in the values of  $X$  for points at the same longitude. The grid-point values of  $X$  and  $Y$  are adjusted, taking account of their reliability, until the residual (algebraic sum of potential differences around each tessera of the grid) are all zero.

(iv) The integral method of Vestine (1941) is applied to the  $Z$  and the adjusted  $X$  and  $Y$  grid-point values to separate the internal and external parts of the potential.

The relative merits of the Price–Wilkins method and the form of spherical harmonic analysis used here for the representation of  $L$  are now discussed under the same headings, (i) to (iv).

(i) The  $L$  data from Chapman–Miller analysis (tables 1 to 3) are in the form of harmonic coefficients, which may readily be subjected to spherical harmonic analysis (§ 4.2). However, values for specified epochs of U.T., suitable for Price–Wilkins analysis, could readily be synthesized.

(ii) If it is necessary to interpolate from the observatories to a grid before analysis, the Price–Wilkins method is probably the best, but inevitably some information is lost in the process. The drawing of loci may be permissible for  $S$ , where the geographical distribution of the variations is reasonably well known, but for  $L$  it would be far too subjective, giving the analyst too much scope for imposing his own ideas. If, as is subsequently shown, the  $L$  current systems tend to follow lines of equal dip, this is here an observational result. Had such a result been obtained by the Price–Wilkins method, it would not be possible to say if this were really a property of  $L$ , or if it merely resulted from the choice of loci.

Although in the past most spherical harmonic analyses have been based on grid-point values, the availability of computers has removed the need for this constraint. In the present analysis, the equations of condition are formed for the position of each observatory, so no interpolation is required.

It has been argued that the Price–Wilkins method could be adapted to a grid defined by the positions of the observatories, but this would greatly complicate the subsequent analysis, and has not yet been done.

(iii) The procedure outlined under this heading (above) is a method for excluding the possibility of a non-potential part of the field (i.e. currents flowing between the earth and the air). This is achieved very simply by spherical harmonic analysis, by analysing  $X$  and  $Y$  simultaneously. The reliability of the various determinations of  $X$  and  $Y$  are taken into account completely objectively by weighting the equations of condition according to the vector probable errors.

(iv) The separation of  $L$  into parts of internal and external origin is achieved with no less rigour and much greater ease by comparing the spherical harmonic coefficients of  $Z$  with the corresponding coefficients of  $(X + Y)$ .

At all stages, spherical harmonic analysis is simpler and more direct than the Price–Wilkins method; what, then, are its disadvantages?

The main disadvantage is that detailed features of the field can be represented only by determining an excessively large number of spherical harmonic coefficients. In the present analysis the number of coefficients that may reasonably be determined is deduced from the data. While there are not sufficient coefficients to represent such a localized feature as the equatorial electrojet, there is little direct evidence of such a feature in the  $L$  data used here. In regions, such as Europe, where many observatories are available, much of the detail is lost, but this is hardly a serious disadvantage for the present study, which attempts to represent only the broad, global features of the morphology of  $L$ .

Another advantage over spherical harmonic analysis claimed for the Price–Wilkins method is that the model can be adjusted to accommodate new data, without repeating the entire analysis. This is, however, only a theoretical advantage, since it has never been exploited.

#### 4.2. Development

The lunar daily variation of any geomagnetic element at a point may be represented by

$$L = \sum_{n=1}^4 l_n \sin(nt - 2\nu + \lambda_n). \quad (9)$$

Here,  $t$  denotes local mean solar time, measured from local midnight;  $\nu$  is a measure of the phase of the moon, increasing from 0 h at one new Moon to 24 h at the next ( $\nu = t - \tau$ ; cf. equation (3)); and  $l_n, \lambda_n$  are harmonic constants determined from a Chapman–Miller analysis of the observed data. These constants differ for each element, and may be distinguished by adding in parentheses the element to which they refer, e.g.  $l_3(X), \lambda_2(Z)$ . Since we are here concerned with the ionospheric part of  $L$ , the contribution of the ocean effect must be removed. This is done by replacing  $(l_2, \lambda_2)$  with  $(l_I, \lambda_I)$  obtained from equations (6). Similarly,  $\rho_2$  is replaced with  $\rho_I$ , also given by (6).

We will assume that  $(l_2, \lambda_2)$  has been replaced by  $(l_I, \lambda_I)$ , and  $\rho_2$  by  $\rho_I$ , but for mathematical convenience will retain the notation of equation (9), which now refers solely to the ionospheric part of  $L$ .

For a worldwide representation of  $L$ , it is necessary to work in terms of Universal Time,  $t^*$ , rather than local time,  $t$ . Then

$$t = t^* + v, \quad (10)$$

where  $v$  denotes longitude, measured east from Greenwich, in hours. Hence

$$L = \sum_{n=1}^4 l_n \sin(nt^* - 2\nu + \lambda_n + nv), \quad (11)$$

$$\text{or} \quad L = \sum_{n=1}^4 [a_n \cos(nt^* - 2\nu) + b_n \sin(nt^* - 2\nu)], \quad (12)$$

$$\text{where} \quad a_n = l_n \sin(\lambda_n + nv) \quad \text{and} \quad b_n = l_n \cos(\lambda_n + nv). \quad (13)$$

At any given epoch of U.T., the  $L$  potential,  $V$ , at a point with spherical coordinates  $(u, v, r)$  may be represented in spherical harmonic form by

$$V = K + R \sum_k \sum_m \{ (c_k^m \cos mv + s_k^m \sin mv) (R/r)^{k+1} + (\gamma_k^m \cos mv + \sigma_k^m \sin mv) (r/R)^k \} P_k^m(\cos u). \quad (14)$$

Here,  $u$  denotes the colatitude (North polar distance),

$r$  denotes the radial distance from the centre of the Earth,

$K$  is an arbitrary constant,

$R$  denotes the radius of a reference sphere, whose centre coincides with that of the Earth,

$c_k^m, s_k^m$  denote the spherical harmonic coefficients associated with the part of  $V$  that originates within the reference sphere,

$\gamma_k^m, \sigma_k^m$  denote the spherical harmonic coefficients associated with the part of  $V$  that originates outside the reference sphere

and  $P_k^m(\cos u)$  denotes the associated Legendre polynomial of degree  $m$  and order  $k$ .

Following the recommendations of the International Association of Terrestrial Magnetism and Atmospheric Electricity (Goldie 1940), Schmidt quasi-normalization is used, so that

$$P_k^m(x) = \frac{1}{2^k k!} \left\{ \frac{\epsilon_m (k-m)! (1-x^2)^{\frac{m}{2}}}{(k+m)!} \right\} \frac{d^{k+m}}{dx^{k+m}} (x^2-1)^k, \quad (15)$$

where  $\epsilon_m = 1$  for  $m = 0$ ;  $\epsilon_m = 2$  for  $m = 1, 2, 3, \dots$

The north ( $X$ ), east ( $Y$ ) and vertically downward ( $Z$ ) components of magnetic intensity are derived from  $V$  as follows:

$$X = \frac{1}{r} \frac{\partial V}{\partial u}, \quad Y = -\frac{1}{r \sin u} \frac{\partial V}{\partial v} \quad \text{and} \quad Z = \frac{\partial V}{\partial r}. \quad (16)$$

That is

$$X = \sum_k \sum_m \{ (c_k^m \cos mv + s_k^m \sin mv) (R/r)^{k+2} + (\gamma_k^m \cos mv + \sigma_k^m \sin mv) (r/R)^{k-1} \} k X_k^m(\cos u), \quad (17)$$

$$Y = \sum_k \sum_m \{ (c_k^m \sin mv - s_k^m \cos mv) (R/r)^{k+2} + (\gamma_k^m \sin mv - \sigma_k^m \cos mv) (r/R)^{k-1} \} k Y_k^m(\cos u), \quad (18)$$

$$Z = - \sum_k \sum_m \{ (c_k^m \cos mv + s_k^m \sin mv) (k+1) (R/r)^{k+2} - (\gamma_k^m \cos mv + \sigma_k^m \sin mv) k (r/R)^{k-1} \} P_k^m(\cos u); \quad (19)$$

where  $k X_k^m(\cos u) = \frac{d}{du} \{ P_k^m(\cos u) \}$  and  $k Y_k^m(\cos u) = \frac{m}{\sin u} P_k^m(\cos u). \quad (20)$

Since all the observatories are on the surface of the Earth, and the Earth is approximately spherical, we may assume that  $r$  is constant. We choose the radius of the reference sphere to be the mean radius of the Earth ( $R = r = 6371.2$  km), so that  $(R/r)^{k+2}$  and  $(r/R)^{k-1}$  in equations (17), (18) and (19) become unity.

The values of  $X$ ,  $Y$  and  $Z$  given in (17) to (19) are the same as those given by (12), for the specific epoch of U.T.,  $t^*$ , to which (17) to (19) refer. Clearly, the values of  $c_k^m$ ,  $s_k^m$ ,  $\gamma_k^m$  and  $\sigma_k^m$  will vary with U.T., and each may be represented as a function of U.T. by an equation of the same form as (12), namely

$$c_k^m = \sum_{n=1}^4 [c_k^m(a_n) \cos(nt^* - 2\nu) + c_k^m(b_n) \sin(nt^* - 2\nu)], \quad (21)$$

similarly for  $s_k^m$ ,  $\gamma_k^m$  and  $\sigma_k^m$ . Substituting these in (17) to (19) and comparing coefficients of  $\cos(nt^* - 2\nu)$  and  $\sin(nt^* - 2\nu)$  with (12) (for  $X$ ,  $Y$  and  $Z$ ), we obtain for each  $a_n(X)$  and  $b_n(X)$  an equation of the same form as (17); for  $a_n(Y)$  and  $b_n(Y)$  equations of the form (18); for  $a_n(Z)$  and  $b_n(Z)$  equations of the form (19).

Each observed value of  $a_n$  gives an equation of condition involving  $c_k^m(a_n)$ ,  $s_k^m(a_n)$ ,  $\gamma_k^m(a_n)$  and  $\sigma_k^m(a_n)$ , and similarly for each  $b_n$ . These equations may be solved by the method of least squares to yield the spherical harmonic coefficients. In practice, for each value of  $n$ , we solve the  $X$  and  $Y$  equations for  $g_k^m$  and  $h_k^m$ , where

$$g_k^m = c_k^m + \gamma_k^m \quad \text{and} \quad h_k^m = s_k^m + \sigma_k^m; \quad (22)$$

and the  $Z$  equations for  $g_k^m$  and  $h_k^m$ , where

$$g_k^m = \left( c_k^m - \frac{k}{k+1} \gamma_k^m \right) \quad \text{and} \quad h_k^m = \left( s_k^m - \frac{k}{k+1} \sigma_k^m \right). \quad (23)$$

The internal and external spherical harmonic coefficients are then separated as follows:

$$\left. \begin{aligned} c_k^m &= [k g_k^m + (k+1) g_k^m] / (2k+1), \\ s_k^m &= [k h_k^m + (k+1) h_k^m] / (2k+1), \\ \gamma_k^m &= (g_k^m - g_k^m) (k+1) / (2k+1), \\ \sigma_k^m &= (h_k^m - h_k^m) (k+1) / (2k+1). \end{aligned} \right\} \quad (24)$$

The significance of the lunar vectors  $(l_n, \lambda_n)$  varies from station to station, and for different magnetic elements and values of  $n$ . Since we have a measure of the significance of each  $(l_n, \lambda_n)$  in its vector probable error,  $\rho_n$ , we use this measure to weight the equations of condition before solving for the spherical harmonic coefficients. Following standard statistical practice, each equation of condition is multiplied by  $1/\rho_n$ , so that its contribution to the normal equations is proportional to  $1/\rho_n^2$ .

Standard deviations of the spherical harmonic coefficients  $g_k^m, h_k^m, g_k'^m, h_k'^m$  are deduced from  $Q$ , the sum of the squares of the residuals from the weighted equations of condition, and  $W_k^m$ , the weights of the unknowns as indicated by the coefficients of the leading diagonal of the inverse of the normal equation matrix,

$$\text{standard deviation} = \left( \frac{QW_k^m}{N-M} \right)^{\frac{1}{2}}. \quad (25)$$

Here,  $N$  denotes the number of equations of condition and  $M$  denotes the number of unknowns evaluated from the equations.

#### 4.3. *The spherical harmonic analysis*

The number of unknowns that can be significantly determined is not immediately obvious. The greater the value of  $M$ , the closer will be the fit to the initial data, and the smaller will be the value of  $Q$ . In the limiting case when  $M = N$ , an exact fit will be obtained, and  $Q$  will be zero. However, as  $M$  increases, the denominator of (25) decreases (to zero in the limiting case), with a consequent increase in the standard deviation. For this reason, a number of pilot analyses was performed and it was concluded that, for the  $Z$  analysis, it is reasonable to determine 20 to 30 unknowns. For the  $X + Y$  analysis, more values may be determined (since twice as many equations of condition are available), however, we are concerned with the evaluation of internal and external parts of the  $L$  potential, and for each internal or external spherical harmonic coefficient we require the corresponding coefficient from both the  $X + Y$  and  $Z$  analysis. Moreover, an examination of equations (24) shows that the contribution of the  $Z$  coefficients to the internal and external coefficients is never less than that from the  $X + Y$  coefficients.

Having decided on the number of harmonic coefficients to be determined, we still have to decide which harmonics these should be. In the spherical harmonic expansion of the main field, the harmonic amplitudes decrease fairly steadily with increasing  $k$ , so it is usual to determine all the harmonics up to a chosen value of  $k$ ; however, the distribution of the variation field amplitudes with  $m$  and  $k$  differs from that of the main field amplitudes, so different considerations apply. Very little is known of the distribution of the variation field amplitudes, so as a first approach the data were analysed for all harmonics up to  $m = k = 5$ . The data were then re-analysed, including only the largest of the harmonics from the first analysis and a few higher order harmonics to permit a representation of the rapidly changing effects near the equator. Unfortunately, the revised harmonics differed markedly from the original determinations, some increasing and others decreasing to insignificance. It seems likely that, had some of the previously insignificant harmonics been included, a few of their amplitudes also would have become appreciable. This instability in the solution must be due to poor conditioning of the normal equations matrix, resulting from the poor geographical distribution of data and the relatively low weight given to the results from higher latitudes. Nothing can be done about the geographical distribution, and it would be unreasonable to change the weighting of the higher latitude results, since this is based directly on the quality of the results.



As an aid to deciding which harmonics should be included in the analysis, we may consider the physics of the phenomenon. Viewed from the Sun (or Moon), we would expect the pattern of  $L$  to remain nearly constant for any specific phase of the Moon, with the Earth rotating under it. The reasons for changes in the pattern are the lack of axial symmetry of the Earth's main magnetic field and inhomogeneities in the Earth's conductivity. If these may be ignored,  $L$  is a function of local time and latitude only, and  $l_n$  and  $\lambda_n$  depend only on  $n$  and latitude. It is shown in § 4.4 that, under these assumptions, the expression for the  $L$  potential involves only coefficients of degree  $m = n$ . Since the magnetic and geographical axes do not coincide, there will be some dependence on longitude, and this will produce additional harmonics, probably of smaller amplitude, the main ones being of order  $n \pm 1$ .

TABLE 6. SPHERICAL HARMONIC COEFFICIENTS EVALUATED IN THE PENULTIMATE ANALYSIS OF  $L$

Those retained in the final analysis are shown in parentheses.

$n = 1$	$n = 2$	$n = 3$	$n = 4$
$(g_1^0)$ $(g_1^1 h_1^1)$ $(g_2^0)$ $(g_2^1 h_2^1)$ $(g_2^2 h_2^2)$ $(g_3^0)$ $(g_3^1 h_3^1)$ $(g_3^2 h_3^2)$ $(g_4^1 h_4^1)$ $g_5^1 h_5^1$ $g_6^1 h_6^1$ $g_7^1 h_7^1$ $g_8^1 h_8^1$	$(g_1^1 h_1^1)$ $(g_2^1 h_2^1)$ $(g_2^2 h_2^2)$ $(g_3^1 h_3^1)$ $(g_3^2 h_3^2)$ $(g_3^3 h_3^3)$ $(g_4^1 h_4^1)$ $(g_4^2 h_4^2)$ $(g_4^3 h_4^3)$ $g_5^2 h_5^2$ $g_6^2 h_6^2$ $g_7^2 h_7^2$ $g_8^2 h_8^2$	$(g_2^2 h_2^2)$ $(g_3^2 h_3^2)$ $(g_3^3 h_3^3)$ $(g_4^2 h_4^2)$ $(g_4^3 h_4^3)$ $(g_4^4 h_4^4)$ $g_5^2 h_5^2$ $(g_5^3 h_5^3)$ $g_5^4 h_5^4$ $g_6^3 h_6^3$ $g_7^3 h_7^3$ $g_8^3 h_8^3$	$(g_3^3 h_3^3)$ $(g_4^3 h_4^3)$ $(g_4^4 h_4^4)$ $(g_5^3 h_5^3)$ $(g_5^4 h_5^4)$ $(g_5^5 h_5^5)$ $g_6^3 h_6^3$ $(g_6^4 h_6^4)$ $g_6^5 h_6^5$ $g_7^4 h_7^4$ $g_8^4 h_8^4$

In the light of these considerations, a new analysis was made in which the harmonics determined were those of degree  $n$  and order  $k$ , where  $k$  takes values from  $n$  to 8, and those of degree  $n \pm 1$  and order  $n - 1$  to  $n + 2$ . These are listed in table 6. This set of harmonics has the advantage of including all the larger harmonics determined empirically in the earlier analyses.

The higher harmonics were included to permit the representation of the enhanced  $L$  variations in  $X$  observed near the equator (e.g. at Huancayo, Addis Ababa and Kodaikanal). These variations presumably result from an electrojet effect, analogous to that familiar in studies of  $S$ . However, there is no direct evidence that this effect in  $L$  is limited to a band only a few degrees wide, as it is in  $S$ . If it were, its representation would require harmonics of much higher order than 8, which it would be unrealistic to attempt to determine from the present data set.

An examination of the spherical harmonic coefficients obtained from this analysis showed that, although several of the higher harmonics had appreciable amplitudes, very few of these were significantly determined. This shows that, although an electrojet effect may be present, the distribution and reliability of the data used in this study are not adequate to show this feature significantly. With the objective of obtaining the most compact model that adequately represents the data, a final analysis was made from a more restricted set of coefficients (those in parentheses in table 6).

The final set of coefficients from the analysis of  $X + Y$  and  $Z$  is given in table 7 in units of 0.001 nT. Although a few of the standard deviations are slightly greater than those obtained in the previous analysis, the majority of them are smaller, particularly for the  $Z$  analysis, and they tend to decrease more rapidly with increasing order, indicating that we now have a more stable solution. None of the final coefficients differs significantly from the corresponding coefficient determined in the previous analysis, giving further evidence of stability.

TABLE 7. SPHERICAL HARMONIC COEFFICIENTS FROM ANALYSIS OF  $X+Y$  AND  $Z$ 

Unit = 0.001 nT

		X+ Y analysis			Z analysis		
m	k	g or h	a	b	g' or h'	a	b
n = 1							
0	1	g	79± 77	90± 64	g'	-49± 54	81± 58
1	1	g	-45 63	-71 52	g'	29 35	71 38
1	1	h	92 61	190 51	h'	46 42	10 45
0	2	g	-151 60	15 50	g'	65 38	-28 41
1	2	g	42 61	-515 51	g'	-89 40	86 43
1	2	h	-429 63	149 53	h'	92 44	-56 48
2	2	g	6 44	-48 37	g'	181 32	82 34
2	2	h	-254 47	57 39	h'	-66 32	-8 34
0	3	g	53 48	60 40	g	-121 40	21 43
1	3	g	-48 48	-68 40	g'	-45 33	-51 36
1	3	h	-101 56	-7 47	h'	-69 38	-1 41
2	3	g	5 38	18 31	g	-67 26	-10 28
2	3	h	109 40	23 34	h'	52 27	-6 29
1	4	g	57 34	249 28	g	32 29	-91 31
1	4	h	241 43	8 36	h'	36 30	-19 32
n = 2							
1	1	g	-225± 109	-118± 87	g'	-158± 55	-101± 61
1	1	h	-171 98	25 78	h'	71 76	-170 85
1	2	g	59 99	22 78	g'	95 62	-83 69
1	2	h	80 98	30 78	h'	-70 79	21 88
2	2	g	118 73	-99 58	g'	-69 48	-210 53
2	2	h	81 75	-17 60	h'	63 52	115 57
1	3	g	125 77	29 61	g'	-4 54	184 60
1	3	h	-190 86	-249 68	h'	97 59	155 65
2	3	g	170 69	790 55	g'	107 46	-115 51
2	3	h	613 73	-47 58	h'	-219 50	-10 55
3	3	g	69 58	226 46	g'	27 39	-59 44
3	3	h	142 61	18 49	h'	27 36	204 40
1	4	g	-143 50	-52 40	g'	83 42	-62 46
1	4	h	-94 64	-5 51	h'	-54 41	-94 46
2	4	g	-52 58	-114 46	g'	-2 37	87 41
2	4	h	-71 56	-80 44	h'	51 39	-58 43
3	4	g	78 51	33 40	g'	-26 31	-27 34
3	4	h	-110 49	11 39	h'	-16 29	-95 32
n = 3							
2	2	g	149± 35	171± 42	g'	-21± 27	24± 26
2	2	h	188 33	-148 40	h'	-65 26	-56 24
2	3	g	-101 33	-72 40	g'	-8 23	44 22
2	3	h	-66 31	-13 37	h'	17 22	22 22
3	3	g	-91 28	-62 34	g'	-8 21	-4 20
3	3	h	-47 27	-76 32	h'	39 26	-52 25
2	4	g	33 26	-8 31	g'	-10 20	-52 19
2	4	h	44 24	42 30	h'	-12 17	44 16
3	4	g	-42 30	-228 36	g'	-6 18	65 17
3	4	h	-322 25	-101 30	h'	55 24	11 24
4	4	g	-40 21	-45 25	g'	0 22	-20 22
4	4	h	-68 25	54 30	h'	77 18	-2 17
3	5	g	-24 22	64 27	g'	3 17	-6 16
3	5	h	55 20	0 24	h'	-27 17	3 16
n = 4							
3	3	g	-23± 16	-57± 17	g'	11± 7	22± 8
3	3	h	-18 13	19 14	h'	-19 10	23 11
3	4	g	-32 16	19 16	g'	7 7	-23 8
3	4	h	6 14	26 14	h'	2 8	-11 9
4	4	g	-12 12	12 12	g'	-17 8	10 9
4	4	h	-3 14	-11 14	h'	-8 8	-14 9
3	5	g	-33 11	24 12	g'	2 6	10 6
3	5	h	2 12	1 12	h'	13 6	1 6
4	5	g	6 12	37 12	g'	2 6	-10 7
4	5	h	84 14	4 14	h'	-11 7	-10 8
5	5	g	38 11	-10 12	g'	-8 6	-28 7
5	5	h	23 10	-21 11	h'	-11 7	-14 8
4	6	g	4 10	-13 10	g'	9 5	12 6
4	6	h	-13 11	-14 11	h'	14 5	9 6

TABLE 8. SPHERICAL HARMONIC COEFFICIENTS OF THE INTERNAL AND  
 EXTERNAL PARTS OF THE  $L$  FIELD

Unit = 0.001 nT							
m	k	Internal			$\gamma$ or $\sigma$	External	
		c or s	a	b		a	b
n = 1							
0	1	c	-6±63	84±60	$\gamma$	85±77	6±71
1	1	c	4 46	24 43	$\gamma$	-49 59	-95 53
1	1	s	61 49	70 47	$\sigma$	31 60	120 56
0	2	c	-21 48	-11 45	$\gamma$	-130 55	26 50
1	2	c	-37 49	-154 46	$\gamma$	79 57	-361 52
1	2	s	-116 52	26 50	$\sigma$	-313 60	123 55
2	2	c	111 37	30 35	$\gamma$	-105 42	-78 39
2	2	s	-141 39	18 36	$\sigma$	-113 44	39 40
0	3	c	-46 44	38 42	$\gamma$	99 47	22 44
1	3	c	-46 40	-58 38	$\gamma$	-2 44	-10 41
1	3	s	-83 47	-4 44	$\sigma$	-18 51	-3 47
2	3	c	-36 32	2 29	$\gamma$	41 35	16 32
2	3	s	76 33	6 31	$\sigma$	33 36	17 34
1	4	c	43 31	60 30	$\gamma$	14 33	189 31
1	4	s	127 36	-7 34	$\sigma$	114 39	15 36
n = 2							
1	1	c	-180±77	-107±71	$\gamma$	-45±100	-11±87
1	1	s	-10 84	-105 83	$\sigma$	-161 101	130 94
1	2	c	81 79	-41 73	$\gamma$	-22 90	63 81
1	2	s	-10 87	25 84	$\sigma$	90 98	5 91
2	2	c	6 59	-166 55	$\gamma$	112 68	67 61
2	2	s	70 62	62 58	$\sigma$	11 71	-79 64
1	3	c	51 65	118 60	$\gamma$	74 71	-89 65
1	3	s	-26 72	-18 66	$\sigma$	-164 79	-231 71
2	3	c	134 57	273 53	$\gamma$	36 63	517 57
2	3	s	138 61	-26 56	$\sigma$	475 67	-21 60
3	3	c	45 48	63 45	$\gamma$	24 53	163 48
3	3	s	76 48	124 44	$\sigma$	66 54	-106 48
1	4	c	-17 46	-58 43	$\gamma$	-126 49	6 45
1	4	s	-72 52	-54 48	$\sigma$	-22 57	49 51
2	4	c	-24 47	-2 43	$\gamma$	-28 51	-112 46
2	4	s	-3 47	-68 43	$\sigma$	-68 51	-12 46
3	4	c	20 41	0 37	$\gamma$	58 44	33 39
3	4	s	-58 39	-48 35	$\sigma$	-52 42	59 38
n = 3							
2	2	c	47±30	83±33	$\gamma$	102±34	88±38
2	2	s	36 29	-93 31	$\sigma$	152 33	-55 36
2	3	c	-48 28	-6 31	$\gamma$	-53 30	-66 35
2	3	c	-19 26	7 29	$\sigma$	-47 29	-20 33
3	3	c	-44 24	-29 27	$\gamma$	-47 26	-33 30
3	3	s	2 26	-62 28	$\sigma$	-49 28	-14 31
2	4	c	9 23	-32 25	$\gamma$	24 24	24 27
2	4	s	13 20	43 23	$\sigma$	31 22	-1 25
3	4	c	-22 24	-65 27	$\gamma$	-20 26	-163 30
3	4	s	-113 24	51 27	$\sigma$	-209 26	50 29
4	4	c	-18 22	-31 23	$\gamma$	-22 23	-14 25
4	4	s	13 21	23 24	$\sigma$	-81 23	31 26
3	5	c	-9 19	26 22	$\gamma$	-15 21	38 23
3	5	s	10 18	2 20	$\sigma$	45 19	-2 21
n = 4							
3	3	c	-4±12	-12±13	$\gamma$	-19±13	-45±14
3	3	s	-19 11	21 12	$\sigma$	1 12	-2 13
3	4	c	-10 12	-4 12	$\gamma$	-22 13	23 13
3	4	s	4 11	5 11	$\sigma$	2 12	21 12
4	4	c	-15 10	11 10	$\gamma$	3 11	1 11
4	4	s	-6 11	-13 11	$\sigma$	3 12	2 12
3	5	c	-14 9	16 9	$\gamma$	-19 9	8 10
3	5	s	8 9	1 9	$\sigma$	-6 10	0 10
4	5	c	4 9	11 10	$\gamma$	2 10	26 10
4	5	s	32 11	-4 11	$\sigma$	52 12	8 12
5	5	c	13 9	-20 10	$\gamma$	25 9	10 10
5	5	s	4 8	-17 9	$\sigma$	19 9	-4 10
4	6	c	7 8	0 8	$\gamma$	-3 8	-13 9
4	6	s	2 8	-2 9	$\sigma$	-15 9	-12 9

The spherical harmonic coefficients of the internal and external parts of the magnetic potential, deduced from those given in table 7 using equations (24), are given in table 8, also in units of 0.001 nT. The standard deviations given in table 8 are deduced from those of table 7 by applying equations (24) to the appropriate variances. The coefficients of table 8 are the main end-product of this paper. They represent by far the most detailed model of the worldwide morphology of  $L$  yet produced, and are based on more data than have previously been used in any such analysis. With the exception of the choice of coefficients to be evaluated, described in this section, the analysis is completely objective, so any information contained in the harmonics is directly related to the initial hourly mean values from which they are derived.

#### 4.4. Comparison with previous analyses

##### 4.4.1. Methods and data

The development of the lunar geomagnetic potential given in §4.2 differs from that of Chapman (1919), outlined below. Chapman assumed that  $(l_n, \lambda_n)$  were functions of geographical latitude only. On this assumption  $\bar{a}_n$  and  $\bar{b}_n$  are functions of latitude only, where

$$\bar{a}_n = l_n \sin \lambda_n; \quad \bar{b}_n = l_n \cos \lambda_n. \quad (26)$$

From equations (13) and (26)

$$\bar{a}_n = a_n \cos nv - b_n \sin nv; \quad \bar{b}_n = b_n \cos nv + a_n \sin nv. \quad (27)$$

Substituting the spherical harmonic expansions of  $a_n$  and  $b_n$  for  $X$ ,  $Y$  and  $Z$  into equations (27), and combining trigonometrical terms involving  $nv$  and  $mv$ , we obtain expressions for  $\bar{a}_n$  and  $\bar{b}_n$  with terms involving  $\cos(m \pm n)v$  and  $\sin(m \pm n)v$ . Since Chapman assumed that  $\bar{a}_n$  and  $\bar{b}_n$  are independent of  $v$ , all terms may be ignored except those involving  $\cos(m - n)v$  when  $m = n$ . This greatly simplifies the expressions. A comparison of the simplified expressions with (17) to (19) shows that they may be derived from a potential function for  $L$  of the form:

$$V = K + R \sum_k \sum_n \{ [A_k^n \cos(nt - 2v) + B_k^n \sin(nt - 2v)] (R/r)^{k+1} \\ + [A_k^n \cos(nt - 2v) + B_k^n \sin(nt - 2v)] (r/R)^k \} P_k^n(\cos u) \quad (28)$$

(cf. equation (14))

Here,

$$\left. \begin{aligned} A_k^n &= \frac{1}{2} [c_k^n(a_n) - s_k^n(b_n)], \\ B_k^n &= \frac{1}{2} [c_k^n(b_n) + s_k^n(a_n)], \\ A_k^n &= \frac{1}{2} [\gamma_k^n(a_n) - \sigma_k^n(b_n)], \\ B_k^n &= \frac{1}{2} [\gamma_k^n(b_n) + \sigma_k^n(a_n)], \end{aligned} \right\} \quad (29)$$

where  $c_k^n(a_n)$ ,  $s_k^n(a_n)$ ,  $\gamma_k^n(a_n)$ ,  $\sigma_k^n(a_n)$  denote values of  $c_k^n$ ,  $s_k^n$ ,  $\gamma_k^n$ ,  $\sigma_k^n$  derived from a spherical harmonic analysis of  $a_n$ ;  $c_k^n(b_n)$ ,  $s_k^n(b_n)$ ,  $\gamma_k^n(b_n)$ ,  $\sigma_k^n(b_n)$  denote values of  $c_k^n$ ,  $s_k^n$ ,  $\gamma_k^n$ ,  $\sigma_k^n$  derived from a spherical harmonic analysis of  $b_n$ .

The terms for which  $k - n$  is even describe the part of  $V$  that is symmetrical about the equator, and those for which  $k - n$  is odd describe the part that is antisymmetrical. By analogy with the potential of the solar daily variations, Chapman assumed that the  $L$  potential for the mean of a year, or for the equinoxes, was antisymmetrical about the equator, and he determined only the first antisymmetrical term for each value of  $n$ , viz.  $A_{n+1}^n$ ,  $B_{n+1}^n$ ,  $A_{n+1}^n$ ,  $B_{n+1}^n$ ,  $n = 1$  to 4. (He also determined the harmonics for which  $k = n$  for the difference between the solstitial values of  $L$ , as a measure of the seasonal variation.) These were then converted to amplitude and phase, and the amplitude ratios and phase differences for the external and internal parts were presented.

The data used by Chapman consisted of values of  $\bar{a}_n$ ,  $\bar{b}_n$  for  $X$ ,  $Y$  and  $Z$ , for each of the three Lloyd seasons, deduced from seven years of observations at five observatories (Manila, Zi-Ka-Wei, Batavia, Pavlovsk and Pola). Thus 105 element-years of observatory data were used in Chapman's analysis (compared with 668 element-years in the present analysis).

The only worldwide representation of  $L$  before that of Chapman was by van Bemmelen (1912, corrected 1913), using only the lunar semidiurnal Fourier coefficients,  $\bar{a}_2$ ,  $\bar{b}_2$  for  $X$ ,  $Y$  and  $Z$  at 15 observatories. van Bemmelen derived only the harmonics for  $n = 2$ ,  $k = 3$ .

A more comprehensive analysis of  $L$  was carried out by Matsushita & Maeda (1965*a*), using  $a_2$  and  $b_2$  for  $H$  and  $Z$  at 32 observatories. They used most of the results of lunar analyses of  $H$  and  $Z$  at individual stations then available, incorporating approximately 550 element years of data. The analysis was confined to the lunar semidiurnal part of  $L$ , since this was the only harmonic available from many of the analyses. The geographical distribution of data was even less satisfactory than for the present analysis, particularly for  $Z$ , where only 17 stations were available, only four of which were in the Southern hemisphere. The distribution of data amongst the observatories was also very irregular, some harmonics resulting from the analysis of 64 years of data and others from less than one year. The  $L$  harmonics for the different stations had been obtained by a variety of methods, some of questionable validity, and for at least one station the significance of the determination had been assessed by a novel and wildly optimistic method. Nevertheless, the data set was the best then available, and represented a vast body of information accumulated over many years by many investigators.

The treatment of the data by Matsushita & Maeda differed markedly from that described in §4.2, and also from that of Chapman described in this section. Their procedure was as follows. First, they assumed that  $(l_2, \lambda_2)$  were functions of *dip* latitude only, and worked throughout in dip latitude,  $\phi$ , where  $2 \tan \phi = \tan I$ , and  $I$  denotes the local value of dip. This assumption is more reasonable than that of Chapman (1919) and van Bemmelen (1912) (who assumed that  $l_2$  and  $\lambda_2$  were functions of *geographical* latitude only), particularly at the equator, but leads to mathematical difficulties, since the other coordinate, local time ( $t$ ), is not distributed uniformly along lines of equal dip latitude. Thus the coordinate system is not orthogonal, and the properties of spherical harmonics that depend on such orthogonality are not valid. This problem becomes more severe with increasing latitude. However, Matsushita and Maeda ignored this difficulty, and it is not clear how closely their model represents a true potential and, consequently, how valid is their separation into parts of internal and external origin. In their coordinate system the magnetic element corresponding to  $X$  is  $H$ , that corresponding to  $Y$  is  $D$ , and  $Z$  remains the same. Matsushita & Maeda analysed only  $H$  and  $Z$ , though they listed also values of  $D$ .

The analysis was based on values  $(l_2, \lambda_2)$  interpolated at  $5^\circ$  intervals of  $\phi$  from smooth curves drawn subjectively through the data points. Since very few data were available in the south, the curves were drawn on the assumption of symmetry about the dip equator for equinoctial months and for the mean of the year. Even so, it is difficult to see how some features of the smoothed curves for  $Z$  were justified, until it is realized that these were assumed to be closely similar in shape to the corresponding  $S$  curves of Matsushita & Maeda (1965*b*) for the quiet days of the I.G.Y. This explains, at least in part, why Matsushita & Maeda found more similarities between  $S$  and  $L$  than have other investigators (e.g. Chapman & Bartels 1940; Green & Malin 1971).

From the interpolated values, Matsushita & Maeda deduced 'spherical' harmonic coefficients corresponding to  $A_k^2$ ,  $B_k^2$ ,  $A_k^3$ ,  $B_k^3$  for  $k = 3, 5, 7, 9, 11$  for the mean of the year combined with the



Lloyd e-season, and for  $k = 2$  to 11 for the Lloyd j- and d-seasons. They also presented a set of coefficients for the year which were the mean of the j-, e- and d-season coefficients. The higher harmonics were included to present the rapidly changing features near the dip equator, but since these features are largely based on corresponding  $S$  features rather than on the  $L$  data, their validity is questionable. The coefficients of Matsushita & Maeda do not correspond exactly with those of Chapman (1919), van Bemmelen (1912) or those from the present analysis, because of the different coordinate system to which they are referred.

In none of the analyses described in this section has any attempt been made to estimate the errors of the spherical harmonic coefficients, nor has any account been taken of the contribution of the ocean effect.

#### 4.4.2. Results

From the coefficients of table 8 that correspond to those determined by Chapman (1919) and van Bemmelen (1912, 1913) have been calculated the amplitude,  $e_k^n$ , and phase constant,  $\epsilon_k^n$ , of the external part of the field, by using equation (29) and the relations

$$e_k^n \cos \epsilon_k^n = A_k^n, \quad e_k^n \sin \epsilon_k^n = B_k^n \quad (30)$$

Similar relations hold for the amplitude,  $i_k^n$ , and phase constant  $\iota_k^n$ , of the internal part of the field. Values of  $e_k^n$  in units of 0.01 nT and  $\epsilon_k^n$  in degrees from the present analysis and from previous analyses are presented in table 9. As noted in §4.4.1, the values of Matsushita & Maeda (1965*a*) are not strictly comparable, since they are referred to a different coordinate system.

The agreement with the previous models is very satisfactory, particularly for the  $n = 2$ , terms, for which the data used here were combinations of  $n = 1, 3$  and 4 harmonics (see equations (6)), and contained no direct measures of the lunar semidiurnal harmonic at all. The amplitude  $e_3^2$  is rather greater than the values obtained by Chapman and van Bemmelen, but this is to be expected, since the present data are for sunspot maximum, whereas their data were for sunspot minimum, and Chapman *et al.* (1971) have shown that the amplitude of  $L$  increases with increasing sunspot number.

For the same harmonics, the ratio of external to internal amplitude,  $e_k^n/i_k^n$ , and the phase difference,  $\epsilon_k^n - \iota_k^n$ , are given in table 10. In addition, the corresponding values for the  $S$  field during the I.G.Y./I.G.C. (see appendix A) are included for comparison in the column headed 'solar'. Since the amplitude ratios and phase lag depend only on the conductivity of the Earth and the frequency of the variation, and the  $S$  frequencies differ only slightly from the  $L$  frequencies, we would expect the  $L$  and  $S$  values to be very similar. Although the  $S$  values are not without error, they should be better determined than the  $L$  values, since the observatory  $S$  data are more reliably determined than those for  $L$ . Again, the present values are found to be in satisfactory agreement both with the earlier analyses and with the  $S$  values. The amplitude ratios, as expected, decrease steadily with increasing frequency, unlike those of Chapman, which have a minimum for  $n = 2$ . This low value (and that of van Bemmelen) is probably the result of including the ocean effect with the ionospheric part of  $L_2$ , and thus deducing a larger value for the internal part of the field than would have been obtained from the ionospheric effect alone. The amplitude ratio is critically dependent on the results of the  $Z$  analysis and, since their data for  $Z$  were rather poor, the anomalously high values of the ratio obtained by Matsushita & Maeda are probably not significant. The amount by which the internal part lags behind the external part ( $\iota - \epsilon$ ) is expected to increase with increasing frequency, at least for the low frequencies considered here, and this is

TABLE 9. COMPARISON WITH PREVIOUS ANALYSES: AMPLITUDE AND PHASE ANGLE OF THE EXTERNAL FIELD

$n$	Chapman			Matsushita & Maeda			
	Malin	mean solstice	equinox	van Bemmelen	year	mean solstice	equinox
	$\frac{e_k^n}{0.01\text{nT}}$ deg	$\frac{e_k^n}{0.01\text{nT}}$ deg	$\frac{e_k^n}{0.01\text{nT}}$ deg	$\frac{e_k^n}{0.01\text{nT}}$ deg	$\frac{e_k^n}{0.01\text{nT}}$ deg	$\frac{e_k^n}{0.01\text{nT}}$ deg	$\frac{e_k^n}{0.01\text{nT}}$ deg
1	34	39	36	81	—	—	—
2	34	38	263	42	34	254	271
3	50	273	253	253	58	53	67
4	19	17	22	83	—	—	—
5	4	5	9	280	—	—	—

TABLE 10. COMPARISON WITH PREVIOUS ANALYSIS: AMPLITUDE RATIOS AND PHASE DIFFERENCES FOR THE EXTERNAL AND INTERNAL FIELDS

[illegible]

illustrated by the  $S$  values, although the first of these appears to be improbably low. The lags for  $L$  show a rather erratic behaviour, but it is satisfactory to note that they are all of the right sign, and do not differ greatly from the corresponding  $S$  values.

## 5. THE ASSOCIATED CURRENT FUNCTIONS

### 5.1. Method

As noted in §4.3, the main results of the analysis are summarized by the spherical harmonic coefficients given in table 8. However, the worldwide pattern of  $L$  is not readily visualized from these coefficients, so in this section it is presented graphically, in the form of world charts of the current function,  $J$ .

This function describes the steady electrical currents flowing in a thin spherical conducting shell that would produce the  $L$  variations defined by the spherical harmonic coefficients of the  $L$  potential. The current flows parallel to the lines of equal  $J$ , called current lines, clockwise round a minimum of  $J$  and anticlockwise round a maximum. The current flowing between two current lines for which the current function is  $J_1$  and  $J_2$  is proportional to  $J_1 - J_2$ .

The current function may be obtained from the spherical harmonic coefficients as follows:

$$J = - \sum_k \frac{10}{4\pi} \frac{2k+1}{k+1} \left( \frac{r}{R} \right)^k \sum_m (\gamma_k^m \cos mv + \sigma_k^m \sin mv) P_k^m \quad (r > R), \quad (31)$$

$$J = \sum_k \frac{10}{4\pi} \frac{2k+1}{k} \left( \frac{R}{r} \right)^{k+1} \sum_m (c_k^m \cos mv + s_k^m \sin mv) P_k^m \quad (r < R) \quad (32)$$

(see Chapman & Bartels (1940) and Leaton (1962)). Equation (31) represents the external part of the field as a current flowing in a spherical shell external to the surface of the Earth, and (32) represents the internal part as a current flowing in a shell internal to the surface of the Earth.

We choose  $r/R = 1$  for simplicity. Although the external currents flow at altitudes above 100 km and the internal currents flow at depths of several hundred kilometres,  $J$  is insensitive to such small changes in  $r$ . However, the model is not completely satisfactory because the internal currents are not confined to a thin spherical shell and the external currents flow not only in the ionosphere (which may reasonably well be approximated by a thin shell), but also along lines of force, which extend well out into the magnetosphere. These latter field-aligned currents are now thought to comprise an appreciable proportion of the total external current. For these reasons, the current function diagrams should be considered as a visual aid, rather than as a physical model.

### 5.2. Results

The current function of  $L$  varies with both solar and lunar time, and might best be presented as a computer-produced film. However, it is here presented for a number of specific values of  $t$  and  $\nu$  in figures 3 and 4. For the external part (figures 3*a-f*), the current function is shown for  $\nu = 0$ ;  $t = 0, 6, 12, 18$  h and  $t = 12$  h;  $\nu = 2, 4$ . The patterns for  $\nu = 6, 8, 10$  are the same as those for  $\nu = 0, 2, 4$ , respectively, except that the direction of the current is reversed. For  $\nu = 12, 14, \dots, 22$ , the patterns are identical with those for  $\nu = 0, 2, \dots, 10$ , respectively. The current function for the internal part of the field is of less interest, so it is only shown for  $t = 0$  and 12 h at the epoch of new (or full) moon,  $\nu = 0$  (or 12), in figures 4*a, b*. In all cases the current flowing between adjacent contours is 1000 A, and its direction is indicated by arrows on the contours. The night-

time hemisphere is indicated by shading. The longitude of the mean sun and mean moon are indicated by pictograms below each figure.

For the external part of the  $L$  field, the current function consists of four cells of alternate sign in the Northern hemisphere, uniformly distributed in longitude, and a similar pattern in the Southern hemisphere, with the maxima and minima reversed, so that a Southern minimum is below a Northern maximum. The amplitudes of the cells are enhanced on the sunlit side and diminished (frequently to a point where the cell pattern cannot be distinguished) in the night-time hemisphere. The boundary between the Northern and Southern patterns is approximately aligned with the magnetic equator. The longitude of the 8-cell pattern is controlled by that of the moon, which is always slightly in advance (to the west) of a Northern minimum.

The current function for the internal part of the  $L$  field is essentially similar to that for the external part, but with a smaller amplitude and with the maxima and minima reversed. The phase differences between the internal and external parts of  $L$ , deduced in §4.4.2 (see table 10) imply that the internal current function should be slightly to the West of the external pattern, but this feature is less obvious.

In addition to these broader features, which are all in excellent accord with those predicted by theory, the figures show numerous detailed features. In assessing the reality of these, it is important to consider the distribution of the initial data from which the model was derived. For instance, there are many observatories in Europe, so the pattern there should be well defined, but in the Southern oceans and polar regions, any unusual features are probably spurious.

It is remarkable that such realistic current systems should result from the analysis of only those harmonics ( $L_1$ ,  $L_3$  and  $L_4$ ; see §3.2) that are commonly ignored in the representation of  $L$ , and without imposing any artificial constraints on the model.

### 5.3. *Comparison with earlier current functions*

Very few previous representations of the  $L$  current function have been made. The earliest are given by Chapman & Bartels (1940) (their figures 8.4 to 8.7) for the external part of the field, based on data from five observatories. Since they assumed no dependence on longitude, their abscissae may be considered either as longitude or as lunar time,  $\tau$ . They further assumed anti-symmetry about the Equator. Their figure 8.6, for the equinoxes at new Moon, may be compared with figures 3*a–d* given here. There is a fair degree of agreement; the maxima and minima of Chapman & Bartels are all  $35^\circ$  from the equator, and the mean current flowing between adjacent foci is 10.3 kA, compared with mean values of  $32^\circ$  and 12.3 kA for the present model. It is to be expected that the current for the present model, which is based on data observed at sunspot maximum, should be greater than that of Chapman & Bartels, for sunspot minimum, but no significance can be attached to this difference between the two models.

The external current systems of Matsushita & Maeda (1965*a*) are based solely on the  $L_2$  term, and therefore show no difference between daytime and night-time currents. Nor do they show any variation with longitude. More recently, Matsushita (1969) had adjusted the Matsushita & Maeda model to show day and night differences by introducing assumed values for the diurnal changes in ionospheric conductivity. The resulting external current system for the epoch of new moon is shown in his figure 3. The abscissa is mean lunar time and the ordinate is dip-latitude. For the yearly average, Matsushita finds the dip-latitude of the foci to be  $\pm 20^\circ$ . There is no simple relation between dip-latitude and geographical latitude, but an examination of the iso-clines for  $I = \pm 36^\circ$  (corresponding to dip latitude  $\pm 20^\circ$ ) shows that Matsushita's foci are closer



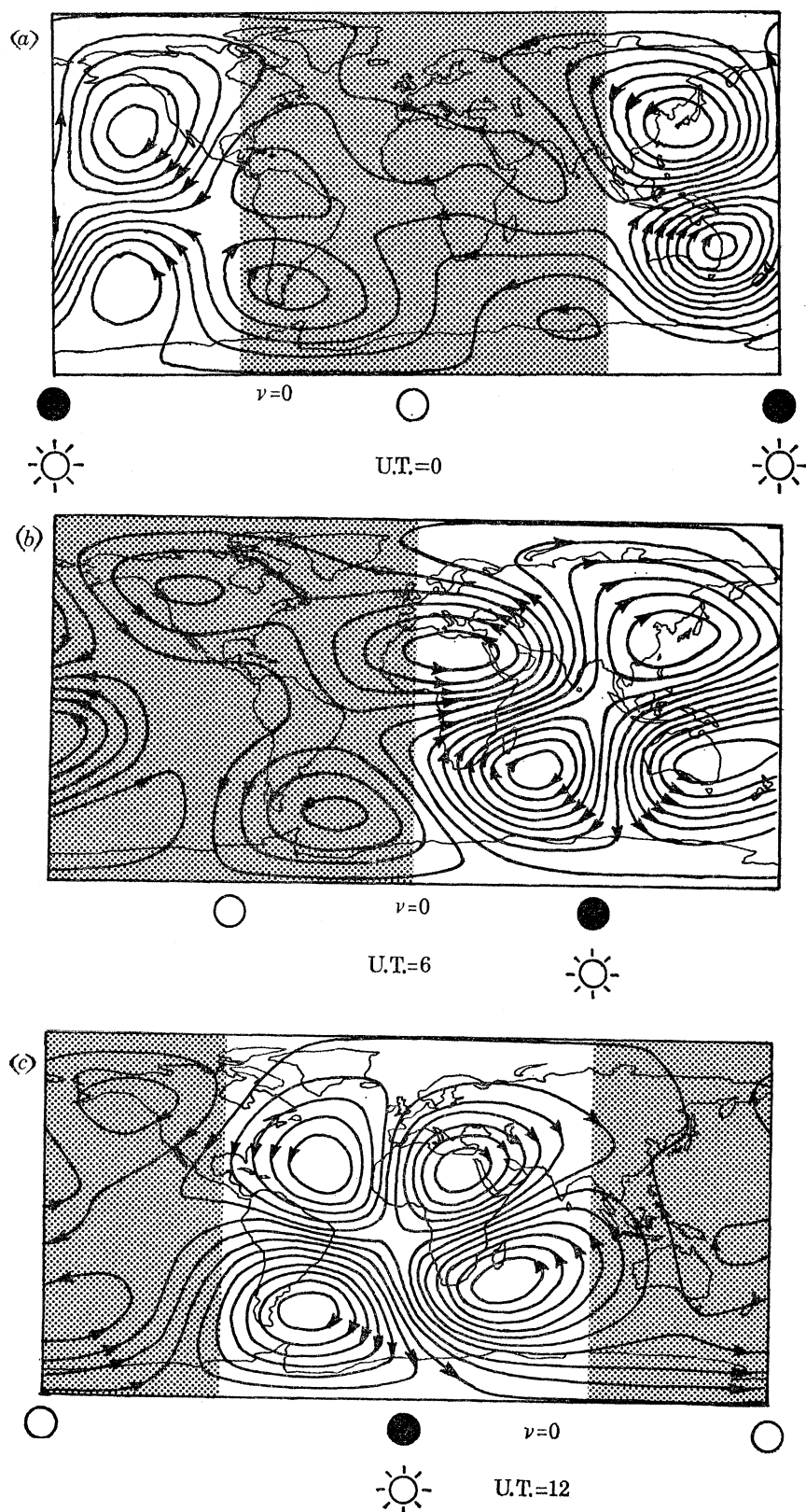
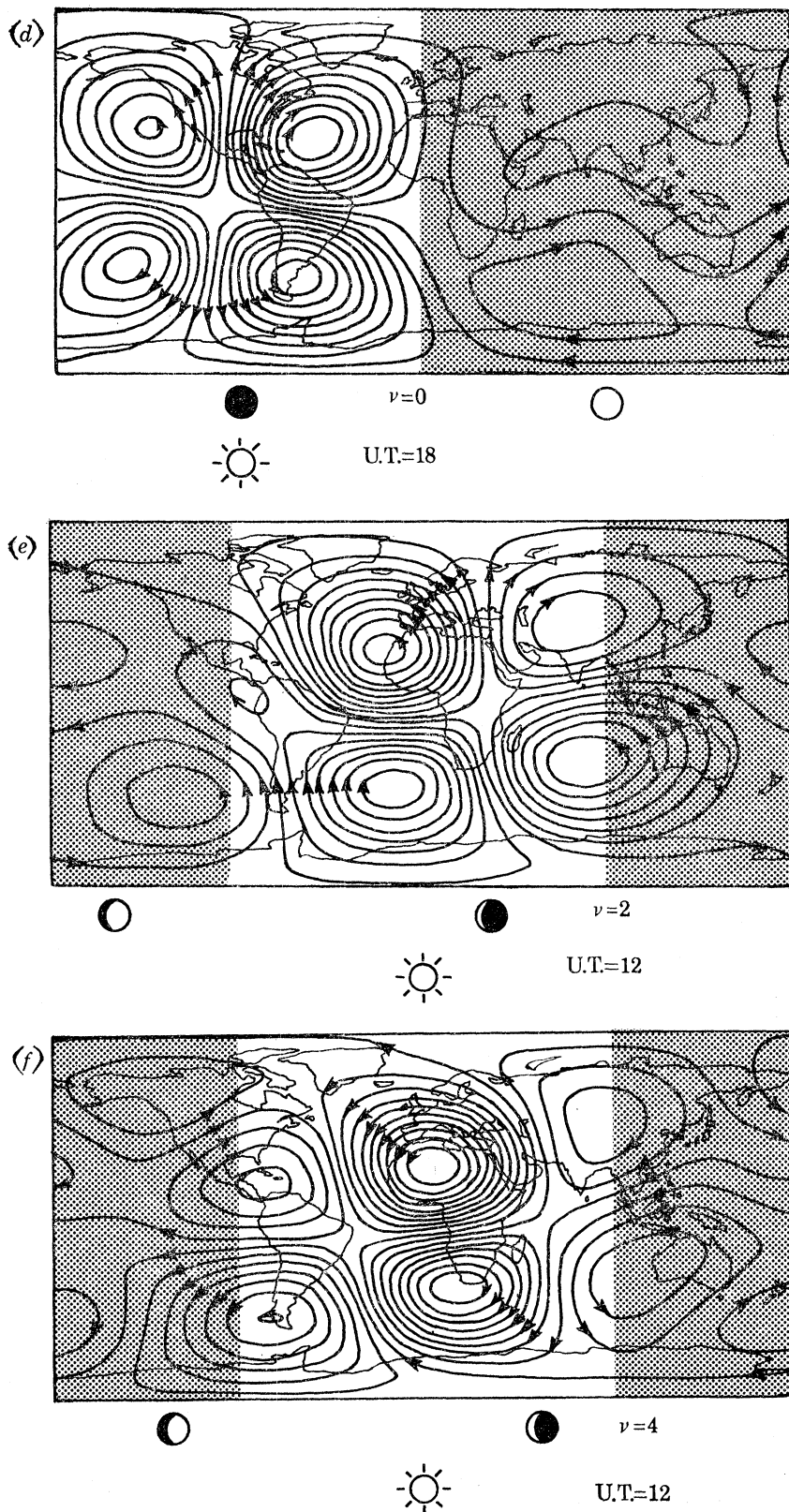


FIGURE 3. For legend see facing page.



FIGURE 3. External current function of  $L$ ; contour interval 1000 A:

- |                              |                              |
|------------------------------|------------------------------|
| (a) U.T. = 0h, $\nu = 0$ h.  | (b) U.T. = 6h, $\nu = 0$ h.  |
| (c) U.T. = 12h, $\nu = 0$ h. | (d) U.T. = 18h, $\nu = 0$ h. |
| (e) U.T. = 12h, $\nu = 2$ h. | (f) U.T. = 12h, $\nu = 4$ h. |

to the equator than is found here. Also, the current between adjacent foci, 17.8 kA is much greater than is found here.

In view of the differences between the present method of deriving current functions and that of Matsushita (1969) (via the model of Matsushita & Maeda 1965*a*; discussed in §4.4.1), the differences between the results are not excessive. Indeed, it is surprising that an analysis of  $L_2$  only, without removal of the ocean contribution, should produce results at all similar to those given here.

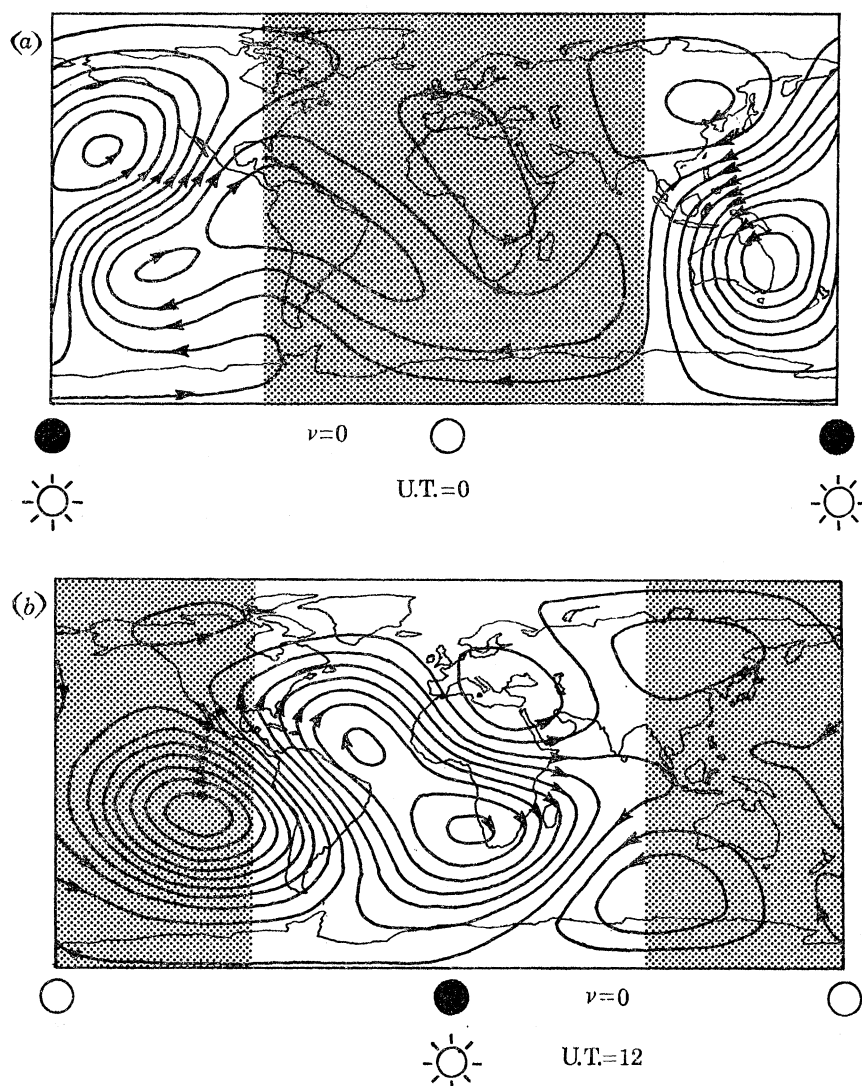


FIGURE 4. Internal current function of  $L$ ; contour interval 1000 A:

(a) U.T. = 0h,  $\nu = 0h$ .

(b) U.T. = 12h,  $\nu = 0h$ .

I am very grateful to Mr B. R. Leaton and the late Professor S. Chapman, F.R.S., for their invaluable guidance and advice. Also to Dr J. C. Gupta who provided the magnetic data in a form suitable for the analysis, Miss Astrik Deirmendjian who assisted with the programming and Mr M. Fisher who prepared the diagrams. Acknowledgement is made to the National Centre for Atmospheric Research, which is sponsored by the National Science Foundation, for computer time used in this research.

# APPENDIX A. SPHERICAL HARMONIC ANALYSIS OF THE SOLAR DAILY GEOMAGNETIC VARIATIONS

The solar and lunar daily geomagnetic variations,  $S$  and  $L$ , are closely related phenomena, and the study of one is complementary to the study of the other. For this reason we here present a spherical harmonic model of the worldwide distribution of  $S$  that may be directly compared with the foregoing  $L$  model. The observatory data are identical with those described in §2.2 and the Fourier harmonics of  $S$  are those deduced as a by-product of the Chapman–Miller analysis (§§2.3 and 2.4). The method of spherical harmonic analysis is closely similar to that of §4.3 (the only differences are those made necessary by the different frequencies of  $S$  and  $L$ ), and the same set of coefficients is evaluated. Thus the results given in this appendix may be directly compared with those for  $L$ .

Besides the advantage of compatibility with the  $L$  model, this analysis has a number of advantages over previous  $S$  analysis. These are:

- (i) More data have been used than previously: 100 observatories, 668 element-years. cf. Matsushita & Maeda (1965*b*): 69 observatories, 138 element-years; W. D. Parkinson (presented at the I.A.G.A. symposium, Potsdam 1970): 64 observatories approximately 220 element-years.
- (ii) The  $S$  data are completely free from contamination by  $L$ .
- (iii) The method of analysis is more objective than has previously been used, involving no hand smoothing or arbitrary weighting.

The spherical harmonic development is as follows (cf. §4.2):

For each observatory and element we have the amplitude,  $s_p$ , and phase constant,  $\sigma_p$ , of the  $p$ th harmonic, for  $p = 1, 2, 3, 4$ , together with the associated vector probable errors, where

$$S = \sum_{p=1}^4 s_p \sin(pt + \sigma_p); \quad (\text{A } 1)$$

or, in Universal Time,  $t^*$ ,

$$S = \sum_{p=1}^4 (a_p \cos pt^* + b_p \sin pt^*), \quad (\text{A } 2)$$

where

$$a_p = s_p \sin(\sigma_p + pv) \quad \text{and} \quad b_p = s_p \cos(\sigma_p + pv). \quad (\text{A } 3)$$

At any given epoch of U.T., the  $S$  potential may be represented in spherical harmonic form by equation (14) from which may be derived values of  $X$ ,  $Y$  and  $Z$  as given in equations (17) to (19). In the case of  $S$ ,

$$c_k^m = \sum_{p=1}^4 [c_k^m(a_p) \cos pt^* + c_k^m(b_p) \sin pt^*], \quad (\text{A } 4)$$

similarly for  $s_k^m$ ,  $\gamma_k^m$ ,  $\sigma_k^m$ . Each observed value of  $a_p$  gives an equation of condition involving  $c_k^m(a_p)$ ,  $s_k^m(a_p)$ ,  $\gamma_k^m(a_p)$ ,  $\sigma_k^m(a_p)$  and similarly for each  $b_p$ . These equations are solved as described in §4.2 to yield the internal and external spherical harmonic coefficients for  $S$  that correspond with the coefficients for  $L$  given in table 8.

The  $S$  coefficients are given in table A 1. The associated current functions are shown in figure A 1 ( $t^* = 0, 6, 12$  and 18 h) for the external part and figure A 2 ( $t^* = 0$  and 12 h) for the internal part. In all cases the current flowing between adjacent contours is 20 kA and its direction is shown by arrows on the contours. The night-time hemisphere is indicated by shading.

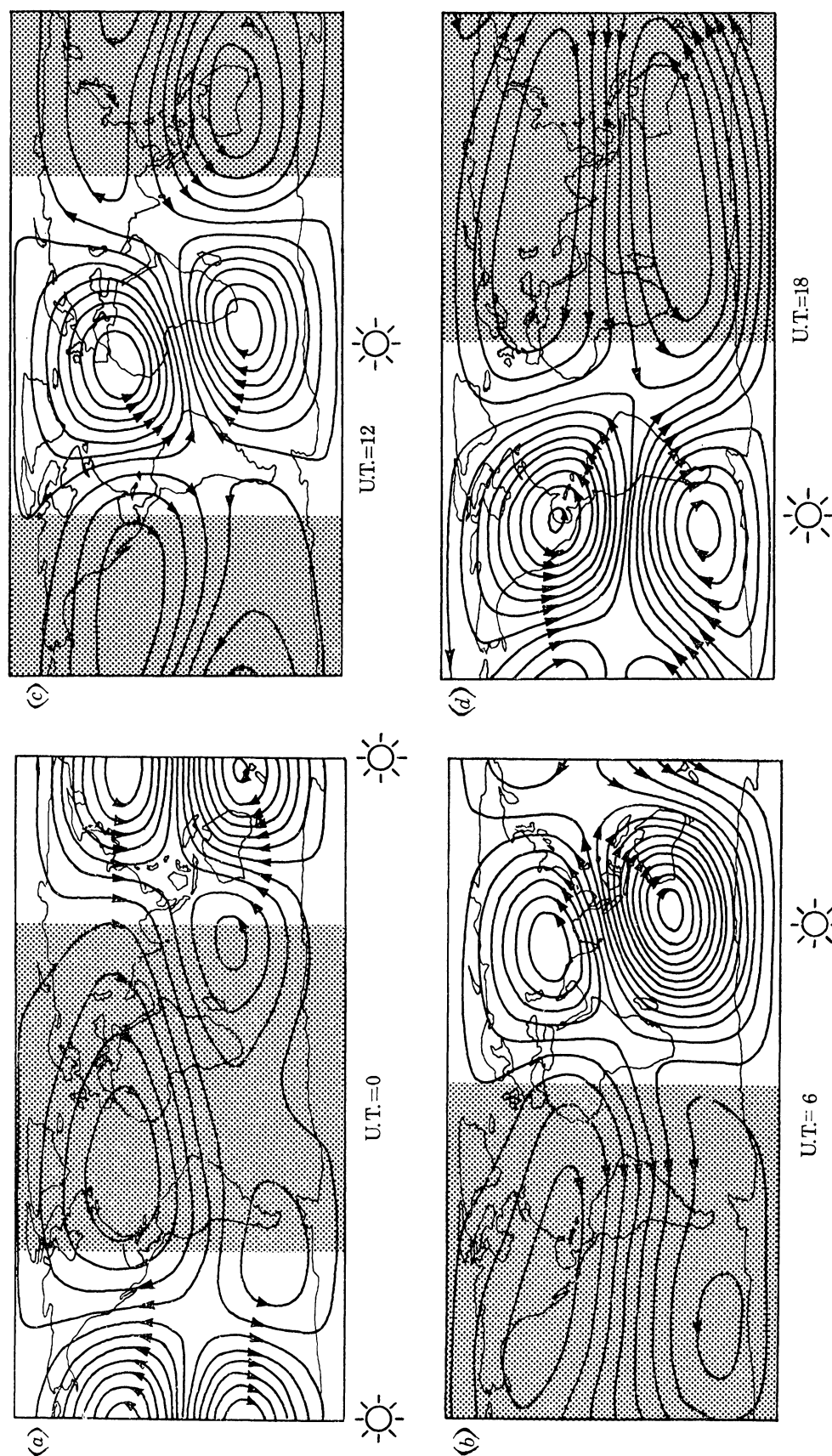
The main difference between the  $L$  and  $S$  current systems is that  $L$  is predominantly semi-

TABLE A1. SPHERICAL HARMONIC COEFFICIENTS OF THE INTERNAL AND EXTERNAL PARTS OF THE  $S$  FIELD

Unit = 0.01 nT

$m$	$k$	internal			external		
		$c$ or $s$	$a$	$b$	$\gamma$ or $\sigma$	$a$	$b$
$p = 1$							
0	1	$c$	$-97 \pm 67$	$-130 \pm 63$	$\gamma$	$60 \pm 94$	$181 \pm 92$
1	1	$c$	$-107 \pm 44$	$-119 \pm 42$	$\gamma$	$151 \pm 68$	$-96 \pm 68$
1	1	$s$	$-113 \pm 51$	$-38 \pm 47$	$\sigma$	$-128 \pm 71$	$-4 \pm 70$
0	2	$c$	$-6 \pm 50$	$-67 \pm 48$	$\gamma$	$28 \pm 65$	$-343 \pm 64$
1	2	$c$	$483 \pm 49$	$-45 \pm 48$	$\gamma$	$1100 \pm 63$	$-154 \pm 62$
1	2	$s$	$-67 \pm 54$	$-410 \pm 52$	$\sigma$	$-162 \pm 69$	$-1321 \pm 68$
2	2	$c$	$-4 \pm 37$	$-78 \pm 35$	$\gamma$	$121 \pm 47$	$-232 \pm 46$
2	2	$s$	$-95 \pm 38$	$-37 \pm 37$	$\sigma$	$-302 \pm 49$	$-124 \pm 48$
0	3	$c$	$24 \pm 47$	$-112 \pm 45$	$\gamma$	$27 \pm 54$	$214 \pm 53$
1	3	$c$	$35 \pm 41$	$-37 \pm 40$	$\gamma$	$-21 \pm 49$	$-29 \pm 48$
1	3	$s$	$76 \pm 48$	$-43 \pm 46$	$\sigma$	$-4 \pm 58$	$190 \pm 57$
2	3	$c$	$30 \pm 32$	$-24 \pm 31$	$\gamma$	$-9 \pm 39$	$62 \pm 37$
2	3	$s$	$-7 \pm 33$	$13 \pm 32$	$\sigma$	$78 \pm 40$	$98 \pm 39$
1	4	$c$	$-93 \pm 34$	$114 \pm 32$	$\gamma$	$-321 \pm 38$	$-156 \pm 37$
1	4	$s$	$40 \pm 39$	$215 \pm 37$	$\sigma$	$-39 \pm 44$	$231 \pm 43$
$p = 2$							
1	1	$c$	$12 \pm 36$	$-72 \pm 30$	$\gamma$	$117 \pm 49$	$-207 \pm 45$
1	1	$s$	$36 \pm 41$	$-8 \pm 32$	$\sigma$	$-217 \pm 52$	$-148 \pm 45$
1	2	$c$	$47 \pm 39$	$59 \pm 31$	$\gamma$	$-62 \pm 44$	$36 \pm 37$
1	2	$s$	$-92 \pm 39$	$-55 \pm 32$	$\sigma$	$-37 \pm 45$	$48 \pm 39$
2	2	$c$	$62 \pm 30$	$76 \pm 25$	$\gamma$	$19 \pm 35$	$98 \pm 31$
2	2	$s$	$22 \pm 25$	$17 \pm 22$	$\sigma$	$154 \pm 31$	$89 \pm 28$
1	3	$c$	$-46 \pm 29$	$46 \pm 24$	$\gamma$	$31 \pm 32$	$79 \pm 27$
1	3	$s$	$41 \pm 31$	$-10 \pm 26$	$\sigma$	$93 \pm 35$	$-71 \pm 31$
2	3	$c$	$-224 \pm 29$	$74 \pm 23$	$\gamma$	$-634 \pm 32$	$9 \pm 27$
2	3	$s$	$83 \pm 25$	$251 \pm 21$	$\sigma$	$31 \pm 29$	$555 \pm 25$
3	3	$c$	$-98 \pm 23$	$51 \pm 18$	$\gamma$	$-77 \pm 25$	$51 \pm 22$
3	3	$s$	$-8 \pm 20$	$-11 \pm 17$	$\sigma$	$127 \pm 23$	$33 \pm 21$
1	4	$c$	$19 \pm 21$	$2 \pm 17$	$\gamma$	$-47 \pm 22$	$-27 \pm 18$
1	4	$s$	$48 \pm 22$	$9 \pm 18$	$\sigma$	$-41 \pm 24$	$73 \pm 21$
2	4	$c$	$-16 \pm 23$	$-25 \pm 19$	$\gamma$	$58 \pm 25$	$23 \pm 21$
2	4	$s$	$-3 \pm 19$	$-61 \pm 17$	$\sigma$	$9 \pm 22$	$-77 \pm 19$
3	4	$c$	$37 \pm 19$	$-8 \pm 16$	$\gamma$	$3 \pm 21$	$-31 \pm 18$
3	4	$s$	$29 \pm 18$	$-29 \pm 15$	$\sigma$	$-48 \pm 20$	$0 \pm 17$
$p = 3$							
2	2	$c$	$-19 \pm 13$	$10 \pm 12$	$\gamma$	$-44 \pm 16$	$38 \pm 15$
2	2	$s$	$11 \pm 13$	$18 \pm 12$	$\sigma$	$7 \pm 16$	$78 \pm 15$
2	3	$c$	$-31 \pm 13$	$1 \pm 11$	$\gamma$	$-22 \pm 15$	$14 \pm 13$
2	3	$s$	$0 \pm 11$	$18 \pm 10$	$\sigma$	$11 \pm 13$	$10 \pm 12$
3	3	$c$	$3 \pm 11$	$-24 \pm 10$	$\gamma$	$2 \pm 13$	$-71 \pm 12$
3	3	$s$	$-5 \pm 11$	$9 \pm 10$	$\sigma$	$-34 \pm 13$	$9 \pm 11$
2	4	$c$	$20 \pm 10$	$-23 \pm 9$	$\gamma$	$22 \pm 11$	$-40 \pm 10$
2	4	$s$	$-30 \pm 9$	$-14 \pm 8$	$\sigma$	$-9 \pm 10$	$-26 \pm 10$
3	4	$c$	$61 \pm 10$	$-56 \pm 9$	$\gamma$	$208 \pm 12$	$-41 \pm 11$
3	4	$s$	$-57 \pm 10$	$-95 \pm 9$	$\sigma$	$-69 \pm 11$	$-207 \pm 10$
4	4	$c$	$7 \pm 10$	$-16 \pm 9$	$\gamma$	$4 \pm 11$	$4 \pm 9$
4	4	$s$	$-17 \pm 9$	$9 \pm 8$	$\sigma$	$-32 \pm 10$	$-22 \pm 9$
3	5	$c$	$1 \pm 8$	$2 \pm 7$	$\gamma$	$-9 \pm 9$	$-10 \pm 8$
3	5	$s$	$-3 \pm 8$	$18 \pm 7$	$\sigma$	$-17 \pm 9$	$7 \pm 8$
$p = 4$							
3	3	$c$	$-3 \pm 4$	$-1 \pm 6$	$\gamma$	$20 \pm 5$	$-13 \pm 7$
3	3	$s$	$-9 \pm 5$	$-10 \pm 6$	$\sigma$	$-7 \pm 5$	$-11 \pm 6$
3	4	$c$	$9 \pm 4$	$-5 \pm 5$	$\gamma$	$-1 \pm 5$	$-6 \pm 6$
3	4	$s$	$0 \pm 4$	$3 \pm 5$	$\sigma$	$-12 \pm 5$	$-1 \pm 6$
4	4	$c$	$6 \pm 4$	$6 \pm 5$	$\gamma$	$1 \pm 5$	$15 \pm 6$
4	4	$s$	$4 \pm 4$	$-14 \pm 5$	$\sigma$	$23 \pm 5$	$3 \pm 6$
3	5	$c$	$-3 \pm 3$	$4 \pm 4$	$\gamma$	$-9 \pm 3$	$4 \pm 5$
3	5	$s$	$9 \pm 3$	$2 \pm 4$	$\sigma$	$11 \pm 3$	$7 \pm 4$
4	5	$c$	$-10 \pm 4$	$15 \pm 5$	$\gamma$	$-37 \pm 5$	$24 \pm 5$
4	5	$s$	$18 \pm 4$	$14 \pm 5$	$\sigma$	$16 \pm 4$	$41 \pm 5$
5	5	$c$	$9 \pm 4$	$-6 \pm 5$	$\gamma$	$7 \pm 4$	$10 \pm 5$
5	5	$s$	$1 \pm 4$	$2 \pm 4$	$\sigma$	$8 \pm 4$	$-6 \pm 5$
4	6	$c$	$2 \pm 3$	$6 \pm 4$	$\gamma$	$4 \pm 3$	$14 \pm 4$
4	6	$s$	$5 \pm 3$	$2 \pm 4$	$\sigma$	$15 \pm 3$	$-1 \pm 4$



FIGURE A 1. External current function of  $S$ ; contour interval 20 kA:

(a) U.T. = 0h.

(b) U.T. = 6h.

(c) U.T. = 12h.

(d) U.T. = 18h.



diurnal, while  $S$  is predominantly diurnal, so only four current cells appear for  $S$ , compared with eight for  $L$ . The amplitude of the  $S$  current, like that of  $L$ , is diminished in the night-time hemisphere. The external daytime pattern is dominated by an anticlockwise cell in the north and a clockwise cell in the south, with their foci at approximately the same longitude as the Sun. Between these foci is a strong east-west current approximately aligned with the magnetic equator. The internal current pattern, like that of  $L$ , is similar to the external pattern, but with reduced amplitude and opposite sign.

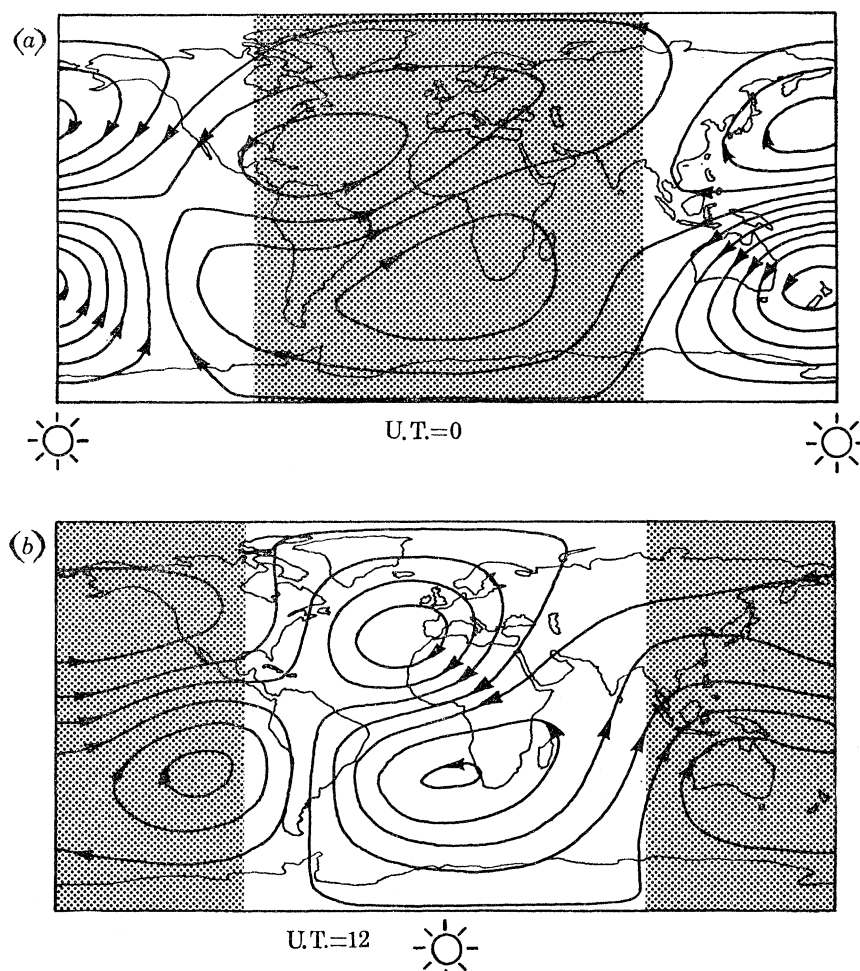


FIGURE A 2. Internal current function of  $S$ ; contour interval 20 kA:

(a) U.T. = 0h.

(b) U.T. = 12h.

The diagrams show an appreciable current flow at local midnight. This is because we have measured  $S$  from the daily mean value as datum, instead of from the quiet night-time level as Price & Wilkins (1963) advocate. By analogy with the treatment of  $L$  (§3), we should measure  $S$  from the synthetic midnight level, and this could readily be done by adding a constant term ( $p = 0$ ) to the Fourier expansion of  $S$  for each station:

$$S = \sum_{p=0}^4 s_p \sin(pt + \sigma_p), \quad (\text{A } 5)$$

where

$$s_0 = - \sum_{p=1}^4 s_p \sin \sigma_p \quad \text{and} \quad \sigma_0 = 90^\circ,$$

so that  $S = 0$  at  $t = 0$ . Spherical harmonic analysis of  $s_0$  would yield an additional set of coefficients for  $p = 0$  to be added to table A 1, and the associated current functions might be expected to be much smaller during the dark hours. However, such an analysis is outside the scope of the present study, and in any case there is still some controversy over the most appropriate datum line for  $S$  (see Matsushita & Maeda 1965*b*).

The present model is for  $S$ , here defined as the mean solar daily variation derived from all except the five *International Disturbed Days* of each month, whereas previous models have been for  $S_q$ , based on the mean for selected quiet days.

#### APPENDIX B. SPHERICAL HARMONIC ANALYSIS OF THE LUNAR SEMIDIURNAL TIDE IN THE ATMOSPHERIC PRESSURE

For an understanding of the processes involved in the ionospheric dynamo, it is necessary to know details of the atmospheric movements at that level. At present, there are insufficient data for a worldwide representation of ionospheric movements. However,  $L_2(p)$ , the variation of atmospheric pressure with the period of  $M_2$ , provides some measure of the response of the atmosphere to the lunar tidal potential, and measures of  $L_2(p)$  are available, deduced from many years of barograph records for a large number of stations with a wide geographical coverage. These data have been collected and subjected to spherical harmonic analysis by Haurwitz & Cowley (1969). Although for many purposes the Haurwitz & Cowley analysis may be considered as definitive, their method of analysis differs in a number of respects from that described in §4 and it is considered desirable to re-analyse their data to produce harmonic coefficients that can be directly compared with those for  $L$  and  $S$  given earlier. Haurwitz & Cowley based their analysis on grid-point values read from subjectively smoothed charts, and deduced a set of spherical harmonic coefficients from the largest Fourier components of the longitudinal variation. They made no direct use of the vector probable errors of the initial data, and gave no numerical estimate of the reliability of the coefficients.

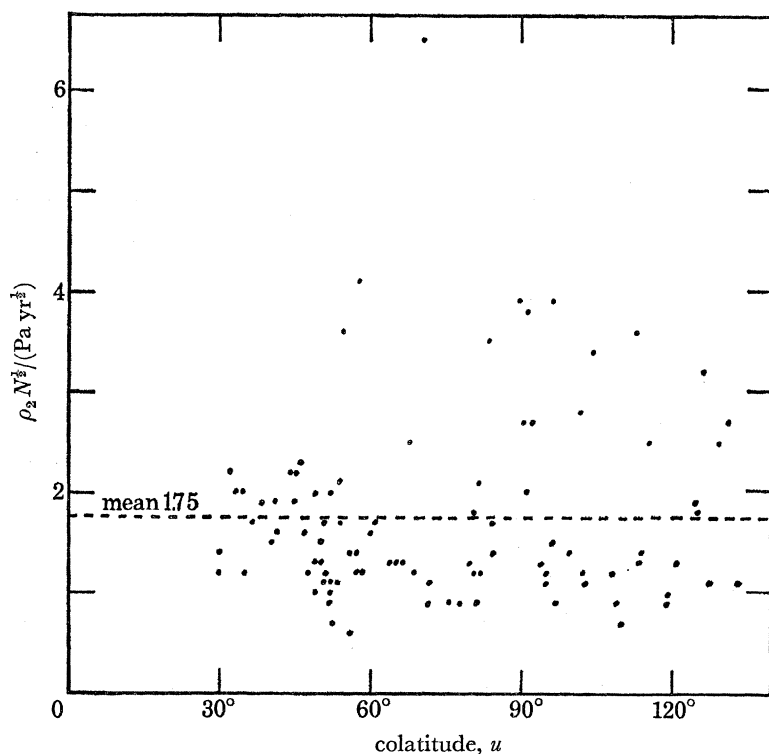
The data for the present analysis are those used by Haurwitz & Cowley (1969) and listed in their Table 1 (pp. 125–127). Several of the 104 stations (Helwan, Mexico City, Bombay, Madras, Perigakulam, Kodaikanal, Singapore, Apia and St Helena) do not have vector probable errors,  $\rho_2$ , associated with the determination of  $L_2(p)$ . In an attempt to estimate these missing values of  $\rho_2$ , values of  $\rho_2 N^{\frac{1}{2}}$ , where  $N$  denotes the number of years of data used in the analysis, are evaluated for the other stations and plotted against colatitude (figure B 1). Although there is some suggestion of variation with colatitude, there is little justification for adopting anything more refined than a simple mean:  $1.75 \text{ Pa yr}^{\frac{1}{2}}$ . For the observatories with no values of  $\rho_2$ , the method of analysis was less refined than that generally used nowadays, so a slightly more pessimistic figure,  $2 \text{ Pa yr}^{\frac{1}{2}}$ , was adopted for estimating likely values of  $\rho_2$  for these. Similar considerations led to the adoption of  $3.3 \text{ Pa yr}^{\frac{1}{2}}$  for the seasons. The resulting values of  $\rho_2$  are listed in table B 1. Thus, for each of 104 stations, we have  $l_2$ ,  $\lambda_2$  and an estimate of  $\rho_2$ .

The lunar semidiurnal variation,  $L_2(p)$  of the surface pressure at each station is given by

$$L_2(p) = l_2 \sin(2t - 2\nu + \lambda_2) = a_2 \cos(2t^* - 2\nu) + b_2 \sin(2t^* - 2\nu). \quad (\text{B } 1)$$

$$\text{Here,} \quad a_2 = l_2 \sin(\lambda_2 + 2\nu) \quad \text{and} \quad b_2 = l_2 \cos(\lambda_2 + 2\nu) \quad (\text{B } 2)$$

(cf. equations (9), (12), (13)).

FIGURE B 1. Variation with colatitude of normalized vector probable errors of  $L_2(p)$ .TABLE B 1. ESTIMATED VALUES OF THE VECTOR PROBABLE ERROR OF  $L_2(p)$ ,  $\rho_2$ , FOR STATIONS WHERE  $\rho_2$  WAS NOT DIRECTLY DETERMINED

station	interval	$N$ yr	$\rho_2$ (annual) Pa	$\rho_2$ (seasons) Pa
Helwan	1900–1908	9	0.67	1.10
Mexico City	1902–1919	18	0.47	0.78
Bombay	1873–1922	50	0.28	0.47
Madras	1841–1860	20	0.45	0.74
Perigakulam	1902–1908	7	0.76	1.25
Kodaikanal	1902–1908	7	0.76	1.25
Singapore	1841–1845	5	0.89	—
Apia	1903–1927	25	0.40	0.66
St Helena	1841–1845	5	0.89	—

It is assumed that the worldwide distribution of  $L_2(p)$  may be represented at any given epoch of U.T. by a spherical harmonic expansion of the form

$$L_2(p) = \sum_m \sum_k (g_k^m \cos mv + h_k^m \sin mv) P_k^m(\cos u). \quad (\text{B } 3)$$

Here,  $g_k^m = g_k^m(a_2) \cos(2t^* - 2\nu) + g_k^m(b_2) \sin(2t^* - 2\nu)$  (B 4)

and  $h_k^m = h_k^m(a_2) \cos(2t^* - 2\nu) + h_k^m(b_2) \sin(2t^* - 2\nu)$ . (B 5)

Values of  $g_k^m(a_2)$ ,  $g_k^m(b_2)$ ,  $h_k^m(a_2)$ ,  $h_k^m(b_2)$  for the same values of  $m$  and  $k$  that were used in the geo-magnetic analyses are derived from the pressure data in a closely similar manner to that for the magnetic analyses; i.e. each observed value provides an equation of condition which is weighted according to  $1/\rho_2$ , and the equations are solved by the method of least squares.



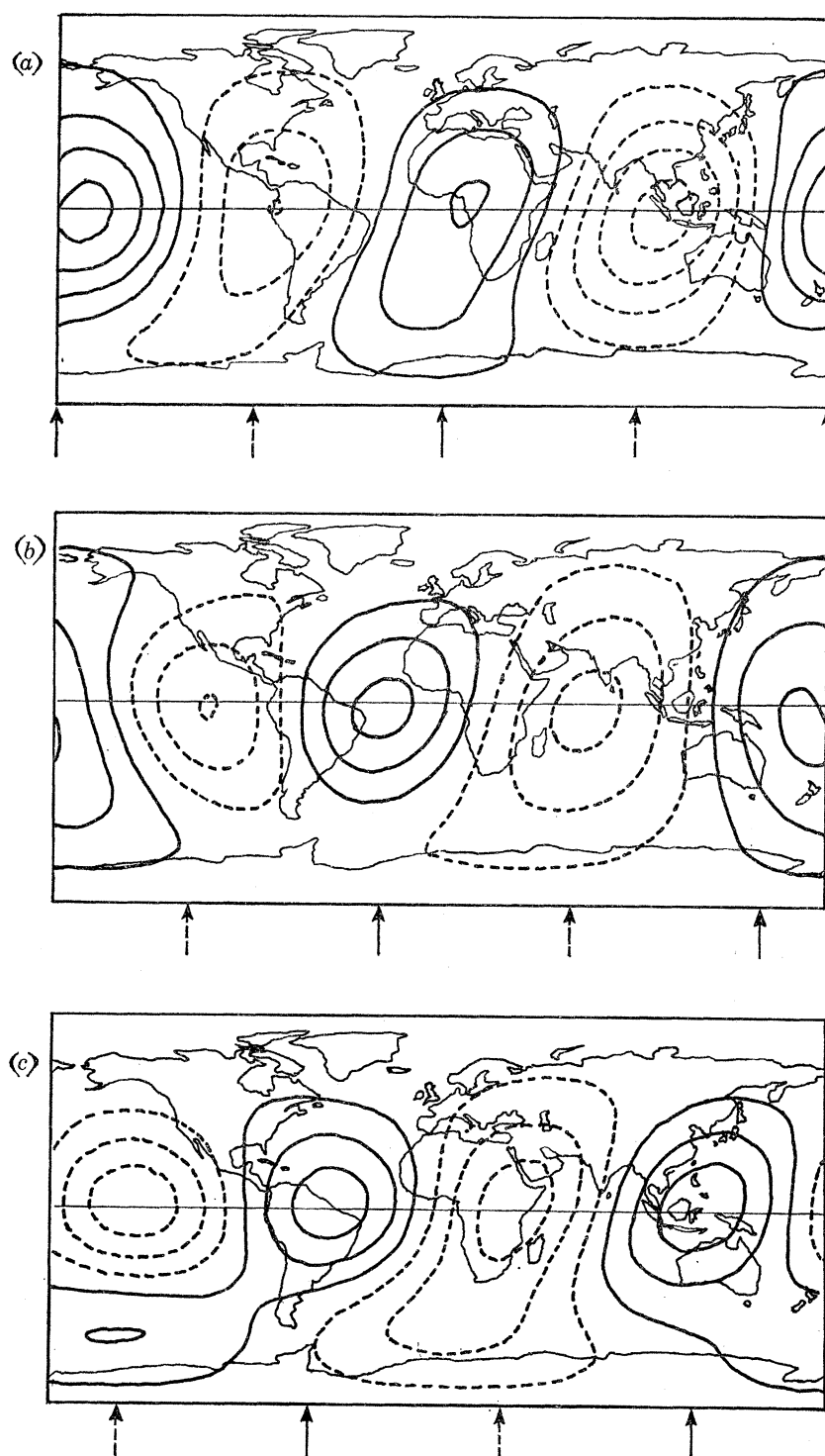


FIGURE B 2. The lunar barometric tide,  $L_2(p)$ ; contour interval 2.0 Pa. Moon's longitude indicated by arrows; for solid arrows the solid contours are positive, for broken arrows the broken contours are positive:

- (a)  $\tau = 0\text{h}$  or  $12\text{h}$  (solid arrows);  $\tau = 6\text{h}$  or  $18\text{h}$  (broken arrows).
- (b)  $\tau = 2\text{h}$  or  $14\text{h}$  (solid arrows);  $\tau = 8\text{h}$  or  $20\text{h}$  (broken arrows).
- (c)  $\tau = 4\text{h}$  or  $16\text{h}$  (solid arrows);  $\tau = 10\text{h}$  or  $22\text{h}$  (broken arrows).



The spherical harmonic coefficients from this analysis are given in table B 2 in units of 0.01 Pa, and the pattern of  $L_2(p)$  is shown for three lunar epochs in figure B 2. The figure shows the annual mean value of  $L_2(p)$  for  $\tau = 0, 2, 4$  h, synthesized by the use of equation (B 3). The contour interval is 2 Pa. The arrows indicate the longitude of the mean moon; for the solid arrows, solid contours are positive and broken contours negative. For the broken arrows, the signs are reversed.

Most of the irregular features occur over the southern oceans, where there are no data to control the model, so these features are probably spurious. The smaller phase lag in the south than in the north may well be real.

Values corresponding to  $a_{2,|s|+m}^s$  and  $b_{2,|s|+m}^s$  of Haurwitz & Cowley (1969) may be deduced from the present values of  $g_k^m(a_2)$ ,  $g_k^m(b_2)$ ,  $h_k^m(a_2)$  and  $h_k^m(b_2)$  as follows:

$$a_{2,|s|+m}^s \equiv \left[ g_{|s|+m}^s(a_2) - \frac{s}{|s|} h_{|s|+m}^s(b_2) \right] (2k+1)^{-\frac{1}{2}}, \quad (\text{B } 6)$$

$$b_{2,|s|+m}^s \equiv \left[ g_{|s|+m}^s(b_2) + \frac{s}{|s|} h_{|s|+m}^s(a_2) \right] (2k+1)^{-\frac{1}{2}}. \quad (\text{B } 7)$$

The main wave ( $s = 2$ ) may be represented by

$$\{56P_2^2 - 5P_4^2\} \sin(2\tau + 73^\circ) + 6P_4^2 \cos(2\tau + 73^\circ) + 6P_3^2 \sin(2\tau + 346^\circ). \quad (\text{B } 8)$$

This may be compared with the result of Haurwitz & Cowley (1969):

$$\{57P_2^2 - 8P_4^2\} \sin(2\tau + 75^\circ) + 5P_4^2 \cos(2\tau + 75^\circ) + 6P_3^2 \sin(2\tau + 326^\circ), \quad (\text{B } 9)$$

and that of Palumbo (1966):

$$\{60P_2^2 - 15P_4^2 + 4P_6^2\} \sin(2\tau + 72^\circ) + 5P_3^2 \sin(2\tau + 341^\circ) + 5P_5^2 \sin(2\tau + 114^\circ). \quad (\text{B } 10)$$

Here, following Haurwitz & Cowley, all the results in the above equations are in the fully normalized form, and the unit is 0.1 Pa.

#### REFERENCES

- Barracough, D. R. & Malin, S.R.C. 1971 *Rep. Inst. geol. Sci.* no. 71/1.  
 Black, D. I. 1970 *Phil. Trans. R. Soc. Lond. A* **268**, 233.  
 Chapman, S. 1914 *Phil. Trans. R. Soc. Lond. A* **213**, 279.  
 Chapman, S. 1919 *Phil. Trans. R. Soc. Lond. A* **218**, 1.  
 Chapman, S. 1952 *Aust. J. sci. Res. A* **5**, 218.  
 Chapman, S. & Bartels, J. 1940 *Geomagnetism*. Oxford: Clarendon Press.  
 Chapman, S., Gupta, J. C. & Malin, S.R.C. 1970 *Beitr. Geophys.* **79**, 5.  
 Chapman, S., Gupta, J. C. & Malin, S.R.C. 1971 *Proc. R. Soc. Lond. A* **324**, 1.  
 Chapman, S. & Kendall, P. C. 1970 *Planet. Space Sci.* **18**, 1597.  
 Chapman, S. & Miller, J. C. P. 1940 *Mon. Not. R. astr. Soc. geophys. Suppl.* **4**, 649.  
 Gauss, C. F. 1839 *Allgemeine Theorie des Erdmagnetismus*. Leipzig.  
 Goldie, A. H. R. (ed.) 1940 *I.A.T.M.E. Bull.* no. 11, 550.  
 Green, Pauline 1972 *Pure Appl. Geophys.* **101**, 194.  
 Green, Pauline & Malin, S. R. C. 1971 *J. atmos. terr. Phys.* **33**, 305.  
 Gupta, J. C. 1968 *NCAR Technical Notes* NCAR-TN-36.  
 Hasegawa, M. 1936 *Proc. imp. Acad. Japan* **12**, 225.  
 Haurwitz, B. & Cowley, Ann D. 1969 *Pure appl. Geophys.* **77**, 122.  
 Leaton, B. R. 1962 *Roy. Obs. Bull.* no. 57.  
 Leaton, B. R., Malin, S. R. C. & Finch, H. F. 1962 *Roy. Obs. Bull.* no. 64.  
 Malin, S. R. C. 1967 *Geophys. J. R. astr. Soc.* **13**, 397.  
 Malin, S. R. C. 1970 *Geophys. J. R. astr. Soc.* **21**, 447.  
 Malin, S. R. C. & Chapman, S. 1970 *Geophys. J. R. Astr. Soc.* **19**, 15.  
 Matsushita, S. 1969 *Radio Sci.* **4**, 771.  
 Matsushita, S. & Maeda, H. 1965a *J. geophys. Res.* **70**, 2559.  
 Matsushita, S. & Maeda, H. 1965b *J. geophys. Res.* **70**, 2535.

- Miller, J. C. P. 1934 *Mon. Not. R. astr. Soc.* **94**, 860.  
Palumbo, A. 1966 *Atti Ass. geofis. ital.* no. 235.  
Pekeris, C. L. & Accad, Y. 1969 *Phil. Trans. R. Soc. Lond. A* **265**, 413.  
Price, A. T. & Wilkins, G. A. 1963 *Phil. Trans. R. Soc. Lond. A* **256**, 31.  
Sastri, N. S. & Rao, D. R. K. 1971 *Geophys. J. R. astr. Soc.* **23**, 269.  
Tschu, K. K. 1949 *Austr. J. sci. Res.* **2**, 1.  
van Bemmelen, W. 1912 *Met. Z.* **29**, 218.  
van Bemmelen, W. 1913 *Met. Z.* **30**, 589.  
Vestine, E. H. 1941 *Terr. Magn. atmos. Elect.* **46**, 27.  
Wilkes, M. V. 1962 *J. atmos. terr. Phys.* **24**, 73.  
Winch, D. E. 1970 *J. Geomagn. Geoelect., Kyoto* **22**, 291.